Supplementary Data

Ratiometric fluorescent probe for sensing Streptococcus mutans glucosyltransferase, a key factor in the formation of dental caries

Lei Feng,[a,b,‡] Qingsong Yan,[a,‡] Baojing Zhang,[a,‡] Xiangge Tian,[a] Chao Wang,*[,a,b] Zhenglong Yu,[a] Jingnan Cui,[b] Dean Guo*[,c], Xiaochi Ma,[a,c] and Tony D. James*[,d]

[a] College of Pharmacy, Academy of Integrative Medicine, The National & Local Joint Engineering Research Center for Drug Development of Neurodegenerative Disease, Dalian Medical University, Dalian 116044, People's Republic of China

[b] State Key Laboratory of Fine Chemicals, Dalian University of Technology, Dalian 116024, China

[c] Chinese Acad Sci, Natl Engn Lab TCM Standardizat Technol, Shanghai Res Ctr Modernizat Tradit Chinese Med, Shanghai Inst Mat Med, Shanghai 201203, China

[d] Department of Chemistry, University of Bath, Bath BA2 7AY, United Kingdom

‡ These authors contributed equally to this work.

Table of Contents

Experimental

Materials and instruments.

All the chemical reagents were purchased from Sigma Aldrich. Recombinant glucosyltransferases was gifted from Professor Jungui Dai of Institute of Materia Medica, Chinese Academy of Medical Sciences and Peking Union Medical College. Human uridine-disphosphate glucuronosyl-transferases (UGT1A7, UGT1A10, UGT2B10, UGT2B11); human Carboxylesterase (CES1b, CES1c, CES2) were purchased from Corning Incorporated Life Sciences. DPP8 peptidase and proteins BSA, HSA were purchased from sigma-aldrich.

NMR spectra were measured using Bruker-600, 500 with tetramethylsilane (TMS) as the internal standard (Bruker, USA). HR-MS data were obtained on an Agilent 1290 infinity 6540 UHD accurate mass Q-TOF MS (Agilent, USA). Constant temperature incubator shaker (ZHWY-2012C) was the production of by Shanghai Zhicheng Analytical Instrument Co. Ltd (P. R. China). Fluorescence microscopic imaging was conducted with Leica Confocal Microscope. The bioassay solutions in 96-well plates were also analysed using a BioTek Synergy H1 microplate reader (BioTek, USA).

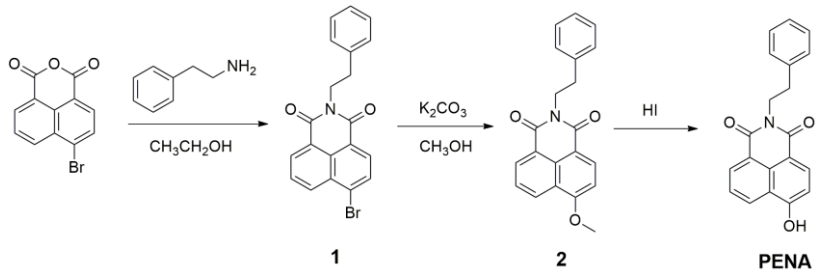

Scheme S1. The synthesis route of fluorescent probe **PENA**.

Synthesis of the fluorescent probe *N*-phenethyl-4-hydroxy-1,8-naphthalimide (PENA)

Synthesis of compound **1**

4-Bromo-1,8-naphthalic anhydride (1 g, 3.62 mmol) and phenylethylamine (0.482 g, 3.98 mmol) were dissolved in ethanol (50 mL). The reaction mixture was stirred and refluxed for 8 h. After cooling to room temperature, the mixture was poured into ice water; the precipitate was isolated, washed with water, and dried to yield 1.25 g of a yellowish-color solid (90.9%).^{1}H NMR (500 MHz, $CDCl_3$) δ 8.67 (d, J = 7.3 Hz, 1H), 8.59 (d, J = 8.5 Hz, 1H), 8.43 (d, J = 7.9 Hz, 1H), 8.06 (d, J = 7.8 Hz, 1H), 7.91 – 7.80 (m, 1H), 7.36 (d, J = 7.4 Hz, 2H), 7.31 (t, J = 7.5 Hz, 2H), 7.23 (t, J = 7.2 Hz, 1H), 4.47 – 4.33 (m, 2H), 3.06 – 2.95 (m, 2H). ^{13}C NMR (125 MHz,$CDCl_3$) δ 163.49, 163.46, 138.65, 133.32, 132.04, 131.23, 131.14, 130.68, 130.32, 129.01, 128.53, 128.11, 126.51, 123.10, 122.23, 41.91, 34.25. HRMS calcd for $C_{20}H_{15}BrNO_2^+$ ($[M+H]^+$) 380.0281, found 380.0276.

Synthesis of compound **2**

A mixture of compound **1** (0.8 g, 2.1 mmol) and K_2CO_3 (2.54 g, 18.4 mmol) in 30 mL CH_3OH was refluxed for 10 h. After cooling to room temperature, excess methanol was removed under reduced pressure and the precipitate was filtered, washed with water and dried to yield compound **2** as a yellow solid (0.593 g, yield: 85.3%). ^{1}H NMR (500 MHz, $CDCl_3$) δ 8.62 (dd, J = 7.3, 0.9 Hz, 1H), 8.58 (d, J = 8.3 Hz, 2H), 7.76 – 7.68 (m, 1H), 7.38 (d, J = 7.2 Hz, 2H), 7.31 (t, J = 7.5 Hz, 2H), 7.22 (t, J = 7.3 Hz, 1H), 7.06 (d, J = 8.3 Hz, 1H), 4.48 – 4.33 (m, 2H), 4.14 (s, 3H), 3.09 – 2.95 (m, 2H). ^{13}C NMR (125 MHz, $CDCl_3$) δ 164.40, 163.82, 160.87, 139.00, 133.45,

129.42, 129.04, 128.69, 128.47, 126.37, 125.97, 123.56, 122.42, 115.11, 105.23, 56.21, 41.71, 34.37. HRMS calcd for $C_{21}H_{18}NO_3^+$ ($[M+H]^+$) 332.1281, found 332.1283.

Synthesis of fluorescent probe *N*-phenethyl-4-hydroxy-1,8-naphthalimide (**PENA**)

A mixture of compound **2** (0.3 g, 0.91 mmol) and 10 mL concentrated HI (55 - 58%) was refluxed for 14 h. After cooling the mixture was poured into water; the precipitate was isolated, washed with water, and dried to yield 0.232 g of the yellow needles solid (80.4%). ^{1}H NMR (500 MHz, DMSO-*d6*) δ 11.89 (s, 1H), 8.56 (d, *J* = 8.3 Hz, 1H), 8.50 (d, *J* = 7.2 Hz, 1H), 8.38 (d, *J* = 8.2 Hz, 1H), 7.82 – 7.76 (m, 1H), 7.38 – 7.25 (m, 4H), 7.25 – 7.13 (m, 2H), 4.30 – 4.17 (m, 2H), 2.96 – 2.86 (m, 2H). ^{13}C NMR (125MHz, DMSO-*d6*) δ 163.56, 162.87, 160.31, 138.82, 133.58, 131.14, 129.19, 128.95, 128.58, 128.42 126.29, 125.62, 122.40, 121.77, 112.54, 109.99, 40.74, 33.60. HRMS calcd for $C_{20}H_{14}NO_3^-$ ($[M-H]^-$) 316.0979, found 316.0986.

Preparation of 4-O-*β*-D-glucopyranosyl-*N*-phenethyl-4-hydroxy-1,8-naphthalimide (PENA-G) by the glucoylation of PENA mediated by fungi *Rhizopus oryzae*.

The filamentous fungi *R. oryzae* was pre-incubated in potato medium to get enough fungi cells for the glucosylation experiment. After filtration, the fungi cells were suspended in the glucosylation medium. The glucosylation medium was sodium phosphate buffer: 13.62 g NaH_2PO_4, 2.36 g NaOH, and 20 g D-glucose in 1000 mL water. 1.5 g *R. oryzae* AS 3.2380 fungus cells were pre-incubated in the glucosylation medium (200 mL), 30 ºC, 130 rpm for 12 h. Then, **PENA** substrates (50 mg) dissolved in acetone were injected into the medium with the continued incubation for 24 h. When the fungus cells were filtered, the incubation culture was subjected to a MCI column, which was eluted by 30% ethanol aqueous, 50% ethanol aqueous, and 95% ethanol, successively. The **PENA** could be obtained in the 50% ethanol aqueous elution with the purity > 95%, the structure of which was determined on the basis of widely spectroscopic data.

The glucosylation of PENA mediated by GTFs and the Glucosyltransferase activity analysis of GTFs by the fluorescent probe PENA.

The fluorescent probe **PENA** was glucosylated by GTFs in the presence of UDPG (300 μM) with the yield of **PENA-G**. The glucosyltransferase (10 μg/mL) was dissolved in 200 μL phosphate buffer (pH 7) together with **PENA** (5 μM) and uridine-diphosphate glucose (UDPG, 300 μM), which was incubated at 37 ºC for 30 min. **PENA** (10 μM) was obtained when the **PENA** stock solution (1 mM, DMSO) was added into the phosphate buffer with the DMSO volume < 1%, which could improve the solubility of **PENA** and keep the activity of GTFs. Then, 100 μL acetonitrile was added to stop the enzymatic reaction. The reaction solutions were measured the fluorescence spectra using BioTek Synergy H1 microplate reader (λ_{ex} 395 nm). The enzymatic reaction solution was analysed for the production of **PENA-G** using HPLC (20%-100% methanol, 0-30 min, flow rate 0.8 mL/min)

Fluorescence responses of **PENA** (5 μM) to the concentration of GTFs were performed upon addition of increasing concentration of GT (0 − 32 μg/mL) in phosphate buffer for 30 min. Meantime, fluorescence responses of **PENA** (5 μM) to the incubation time were studied upon the addition of GTFs (10 μg/mL) in phosphate buffer for incubation time 0 – 80 min with acetonitrile (33%, *v/v*) to terminate the enzymatic reaction (λ_{ex} 395 nm, 37 °C). The relationship was analyzed on the basis of the fluorescence intensities ratio (I_{440}/I_{560}).

The enzymatic selectivity experiments towards different enzymes (10 μg/mL) were preformed according to their enzymatic reaction conditions, including Human uridine-disphosphate glucuronosyl-transferases (UGT1A7, UGT1A10, UGT2B10, UGT2B11); human Carboxylesterase (CES1b, CES1c, CES2), DPP8 peptidase and proteins BSA, HSA.

The fluorescence intensity ratio (I_{440}/I_{560}) was studied on the basis of the fluorescence emission (λ_{ex} 395 nm). The influence of metal ions on the fluorescence emission of **PENA** and **PENA-G** and the activity of GTFs were measured with the presence of K^+, Fe^{3+}, Ba^{2+}, Ca^{2+}, Na^+, Mn^{2+}, Sn^{4+}, Zn^{2+}, Ni^{2+}, Cu^{2+}, Cr^{3+} (each 2 mM). Similarly, the influence of amino acids on the fluorescence intensities of **PENA** and **PENA-G** and the glucosylation capability of GTFs were studied in the presence of various amino acids, such as Ala, Pro, Iso, Phe, Met, Gln, Try, Glu, Asp.

In order to estimate the kinetic parameters of **PENA** for GTFs, the reaction kinetics were performed. Briefly, **PENA** (0−40 μM) was incubated with GTFs for 30 min which ensured less than 20% of substrate was metabolized, and the formation rates of **PENA-G** were in relation to incubation time and protein concentration in the linear range. The **PENA** stock solution was prepared to be 10 mM in DMSO, which was added into the GTFs enzymatic reaction system with DMSO < 1%. The apparent K_m and V_{max} values were calculated from nonlinear regression analysis of experimental data according to the Michaelis-Menten equation.

$$v=\frac{V_{max}\times[S]}{K_m+[S]} \quad \text{.....(1)}$$

The V_{max} represents the maximum rate and K_m is the substrate concentration at the half-maximal rate. Kinetic constants were obtained using Origin 7.5 (origin Lap Corp. Northampton. MA.USA) and produced as the mean ± SD of the parameter estimate.

Confocal laser microscopic imaging of bacteria.

In our work, **PENA** was incubated with seven bacteria strains, including *Streptococcus mutans*, *Hemolytic streptococcus*, *Lactobacillus amylovorus*, *Streptococcus pasteurianus* strain 080205, *Bacillus cereus* 994000168 LBK, *Escherichia coli* DH5alpha BRL, *Staphylococcus aureus* ssp. aureus DSM 3463, to get the fluorescence images by confocal laser scanning microscope. These bacteria were culutred in Luria-Bertani (LB) medium for 24 h to get enuogh bacteria cells with OD value 0.8. Then, **PENA** (50 μM) was subjected into the culture for a co-incubation with bacteria about 1h at 37 ºC. After the clean out of the medium, the bacterial cells were suspended in PBS solution, which were dropped on slide glasses for imaging experiment. The bacteria were imaged using Confocal Microscope with λ_{ex} 405/λ_{em} 415 – 465 nm, λ_{ex} 405/λ_{em} 535 – 585 nm. To study the enzyme specificity, the bacteria were pretreated with enzyme inhibitor **EGCG** (50 μM) and labeled with **PENA** for imaging studies.

Isolated of GTFs inhibitors from green tea.

500 g green tea was extracted with 70% ethanol in water refluxed for 2h. Then, after the evaporation of solvents, the extract was subjected to Waters preparative

HPLC with RP C-18 column for the bioactive fractions preparation. The mobile phase (methanol-water) was assigned as gradient elution for the pre-HPLC. The gradient elution was determined as 10%-20% methanol (0-10 min); 20%-30% methanol (10-40 min); 30%-40% methanol (40-50 min); 40%-100% methanol (50-55 min). For the bioactive fractions with inhibitory effects on GTFs, the main chemical constituents were purified using pre-HPLC again. The structures of isolated compounds were determined on the basis of ^{1}H NMR, ^{13}C NMR and ESI-MS analysis in combination with the literatures. The spectroscopic data of isolated compounds were submitted as followed.

Gallocatechin gallate (GCG). ^{1}H NMR (600 MHz, MeOD) δ 6.97 (s, 2H), 6.39 (s, 2H), 5.95 (s, 2H), 5.38 (q, *J* = 5.2 Hz, 1H), 5.05 (d, *J* = 5.2 Hz, 1H), 4.10 (q, *J* = 7.1 Hz, 1H), 2.74 (qd, *J* = 16.7, 5.1 Hz, 2H), 2.01 (s, 1H), 1.24 (t, *J* = 7.1 Hz, 1H). ^{13}C NMR (150 MHz, MeOD) δ 14.46. 20.85, 23.67, 61.54, 71.06, 79.18, 95.57, 96.36, 99.51, 106.27, 110.13, 121.42, 130.99, 133.94, 139.88, 146.39, 146.98, 156.39, 157.64, 158.12, 167.67, 173.01. (+)-ES-MS *m/z* 459.1 $[M+H]^{+}$, calcd for $C_{22}H_{19}O_{11}^{+}$, 459.0927.

Epigallocatechin gallate (EGCG). ^{1}H NMR (600 MHz, MeOD) δ 6.96 (s, 1H), 6.52 (s, 1H), 5.97 (s, 1H), 5.55 (s, 1H), 3.00 (dd, *J* = 17.2, 4.6 Hz, 1H), 2.86 (dd, *J* = 17.3, 2.4 Hz, 1H). ^{13}C NMR (150 MHz, MeOD) δ 25.44, 48.17, 48.45, 68.53, 77.21, 94.46, 95.10, 98.00, 105.46, 108.84, 120.11, 129.40, 132.38, 138.38, 144.88, 145.28, 155.83, 156.45, 156.49, 166.25. (+)-ES-MS *m/z* 459.1 $[M+H]^{+}$, calcd for $C_{22}H_{19}O_{11}^{+}$ 459.0927.

1,4,6-tri-O-galloyl-*β*-D-glucose (TGG). ^{1}H NMR (600 MHz, MeOD) δ 7.17 (s, 2H), 7.12 (s, 2H), 7.08 (s, 2H), 5.80 (d, *J* = 8.2 Hz, 1H), 5.24 (t, *J* = 9.7 Hz, 1H), 4.46 (dd, *J* = 12.3, 2.0 Hz, 1H), 4.24 (dd, *J* = 12.4, 4.8 Hz, 1H), 4.08 (ddd, *J* = 10.0, 4.7, 2.2 Hz, 1H), 3.86 (t, *J* = 9.3 Hz, 1H), 3.70 – 3.62 (m, 1H). ^{13}C NMR (150 MHz, MeOD) δ 48.17, 62.22, 70.46, 72.89, 73.02, 74.62, 94.43, 108.89, 109.00, 109.20, 119.11, 119.61, 119.75, 138.50, 138.69, 139.07, 145.02, 145.11, 145.15, 165.51, 166.04, 166.65. (+)-ES-MS *m/z* 659.1 $[M+Na]^{+}$, calcd for $C_{27}H_{24}NaO_{18}^{+}$ 659.0860.

Epicatechin gallate (ECG). ^{1}H NMR (600 MHz, MeOD) δ 6.99 – 6.92 (m, 3H),

6.83 (dd, *J* = 8.2, 1.9 Hz, 1H), 6.71 (d, *J* = 8.2 Hz, 1H), 5.98 (t, *J* = 1.9 Hz, 1H), 5.54 (d, *J* = 1.6 Hz, 1H), 5.05 (s, 1H), 3.01 (dd, *J* = 17.3, 4.6 Hz, 1H), 2.87 (dd, *J* = 17.4, 2.1 Hz, 1H). ^{13}C NMR (150 MHz, MeOD) δ 27.47, 50.18, 50.46, 70.57, 79.23, 99.96, 110.79, 115.70, 116.59,119.97, 122.06, 132.06, 140.38, 146.55, 146.57, 146.92, 157.82, 158.40, 158.44, 168.19. (-)-ES-MS *m/z* 441.0 $[M-H]^-$, calcd for $C_{22}H_{17}O_{10}^-$ 441.0822.

Catechin gallate (CG). ^{1}H NMR (600 MHz, MeOD) δ 6.98 (s, 2H), 6.85 (s, 1H), 6.74 (s, 2H), 5.97 (dd, *J* = 9.4, 2.3 Hz, 2H), 5.39 (q, *J* = 5.9 Hz, 1H), 5.08 (d, *J* = 5.9 Hz, 1H), 2.83 (dd, *J* = 16.5, 5.1 Hz, 1H), 2.73 (dd, *J* = 16.5, 6.0 Hz, 1H). ^{13}C NMR (150 MHz, MeOD) δ 166.17, 156.76, 156.25, 155.10, 144.98, 144.93, 144.84, 138.47, 130.11, 119.98, 117.81, 114.81, 113.01, 108.72, 98.23, 95.03, 94.18, 77.94, 69.75, 22.93. (+)-ESI-MS *m/z* 465.1 $[M+Na]^+$, calcd for $C_{22}H_{18}NaO_{10}^+$ 465.0798.

Epigallocatechin (EGC). ^{1}H NMR (600 MHz, MeOD) δ 6.53 (s, 2H), 5.95 (d, *J* = 2.3 Hz, 1H), 5.93 (d, *J* = 2.3 Hz, 1H), 4.77 (s, 1H), 4.19 (t, *J* = 3.0 Hz, 1H), 2.87 (dd, *J* = 16.6, 4.6 Hz, 1H), 2.75 (dd, *J* = 16.7, 2.9 Hz, 1H). ^{13}C NMR (150 MHz, MeOD) δ 156.60, 156.28, 155.92, 145.29, 132.20, 130.12, 105.55, 98.67, 94.94, 94.45, 78.50, 66.12, 27.76. (+)-ESI-MS *m/z* 307.0 $[M+H]^+$, calcd for $C_{15}H_{15}O_7^+$ 307.0818.

Catechin (CA). ^{1}H NMR (600 MHz, MeOD) δ 6.75 (d, *J* = 1.9 Hz, 1H), 6.67 (d, *J* = 8.1 Hz, 1H), 6.63 (dd, *J* = 8.1, 1.9 Hz, 1H), 5.84 (d, *J* = 2.3 Hz, 1H), 5.76 (d, *J* = 2.3 Hz, 1H), 4.47 (d, *J* = 7.5 Hz, 1H), 3.88 (td, *J* = 7.9, 5.5 Hz, 1H), 2.76 (dd, *J* = 16.1, 5.4 Hz, 1H), 2.42 (dd, *J* = 16.1, 8.2 Hz, 1H). ^{13}C NMR (150 MHz, MeOD) δ 156.46, 156.20, 155.53, 144.86, 144.84, 130.81, 118.63, 114.65, 113.84, 99.39, 94.85, 94.07, 81.47, 67.42, 27.14. (+)-ESI-MS *m/z* 291.3 $[M+H]^+$, calcd for $C_{15}H_{15}O_6^+$ 291.2790.

Gallocatechin (GC). ^{1}H NMR (600 MHz, MeOD) δ 6.32 (s, 2H), 5.84 (d, *J* = 2.3 Hz, 1H), 5.77 (d, *J* = 2.3 Hz, 1H), 4.44 (d, *J* = 7.2 Hz, 1H), 3.88 (td, *J* = 7.5, 5.4 Hz, 1H), 2.73 (dd, *J* = 16.1, 5.3 Hz, 1H), 2.42 (dd, *J* = 16.1, 7.8 Hz, 1H). ^{13}C NMR (150 MHz, MeOD) δ 156.44, 156.21, 155.45, 145.46, 132.60, 130.14, 105.76, 99.29, 94.83, 94.08, 81.48, 67.37, 26.71. (+)-ESI-MS *m/z* 329.1 $[M+Na]^+$, calcd for $C_{15}H_{14}NaO_7^+$ 329.0637 .

Epicatechin (ECA). ^{1}H NMR (600 MHz, MeOD) δ 6.99 (d, *J* = 1.9 Hz, 1H), 6.82 (dd, *J* = 8.2, 1.9 Hz, 1H), 6.78 (d, *J* = 8.1 Hz, 1H), 5.96 (d, *J* = 2.3 Hz, 1H), 5.93 (d, *J* = 2.3 Hz, 1H), 4.84 (s, 1H), 4.22 – 4.16 (m, 1H), 2.88 (dd, *J* = 16.7, 4.6 Hz, 1H), 2.76 (dd, *J* = 16.8, 2.8 Hz, 1H). ^{13}C NMR (150 MHz, MeOD) δ 156.62, 156.28, 155.98, 144.55, 144.39, 130.89, 117.98, 114.47, 113.91, 98.65, 94.96, 94.47, 78.48, 66.10, 27.88. (+)-ESI-MS *m/z* 313.1 $[M+Na]^+$, calcd for $C_{15}H_{14}NaO_6^+$ 313.0688.

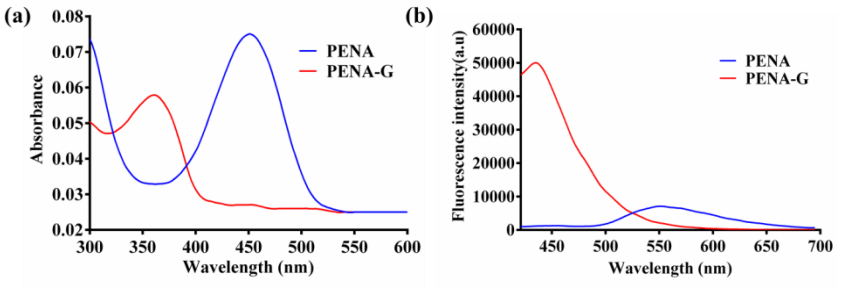

Fig. S1. (a) Absorbance spectra and (b) fluorescence spectra of **PENA** and **PENA-G**, λ_{ex} 395 nm.

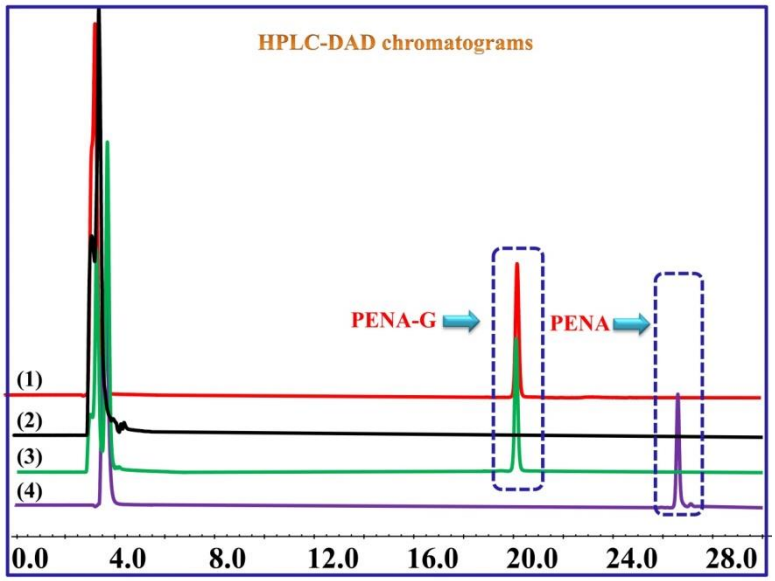

Fig. S2. HPLC-DAD chromatograms of the enzymatic glucosylation of **PENA** mediated by GTFs. (1) Enzymatic reaction solution for the co-incubation of **PENA**, GTFs (10 μg/mL), and UDPG (300 μM). (2) Control solution containing GTFs (10 μg/mL), UDPG (300 μM). (3) Reference **PENA-G**. (4) Reference **PENA**.

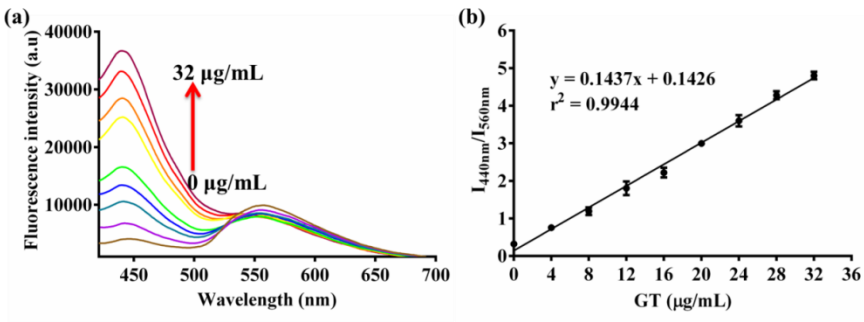

Fig. S3. (a) Fluorescence responses of **PENA** towards GTFs with different concentrations (0 – 32 μg/mL). (b) Linear relationship between fluorescence ratio (I_{440} /I_{560}) and GTFs concentrations (0 – 32 μg/mL). **PENA-G** λ_{ex} 395/λ_{em} 440 nm, **PENA** λ_{ex} 395/λ_{em} 560 nm.

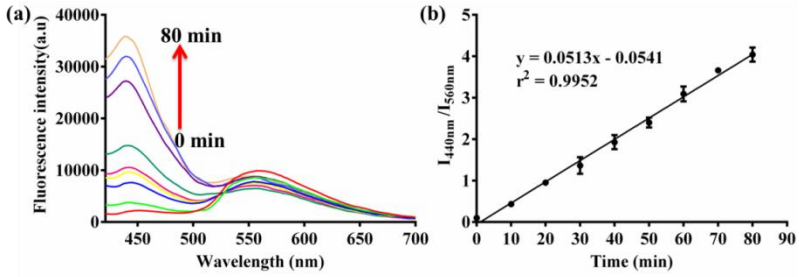

Fig. S4. (a) Fluorescence responses of **PENA** towards GTFs with different incubation time (0 – 80 min). (b) Linear relationship between fluorescence ratio (I_{440}/I_{560}) and incubation time (0 – 80 min). **PENA-G** λ_{ex} 395/λ_{em} 440 nm, **PENA** λ_{ex} 395/λ_{em} 560 nm.

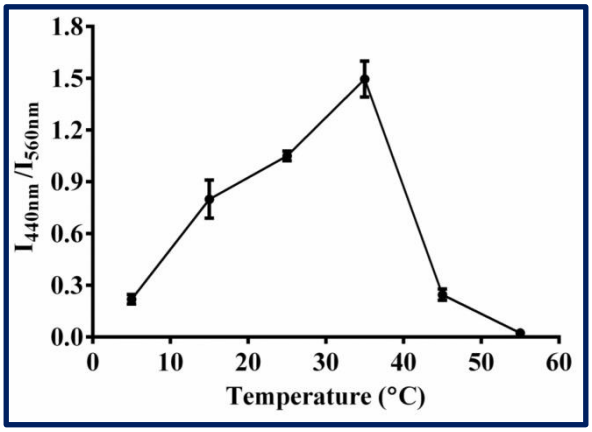

Fig. S5. Glucosylation of **PENA** mediated by GTFs with different incubation temperature (5 – 55 ˚C).

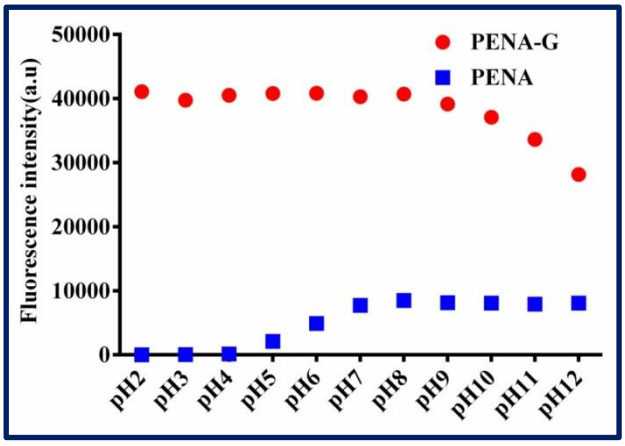

Fig. S6. Fluorescence intensities of **PENA** and **PENA-G** in various PBS solutions with different pH (3 - 12).

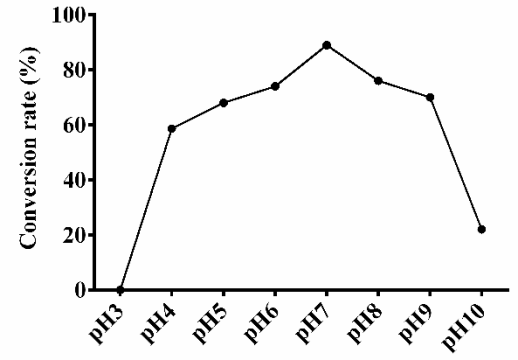

Fig. S7. The conversion rate of **PENA** glucosylation by GTFs in various PBS solutions with different pH conditions.

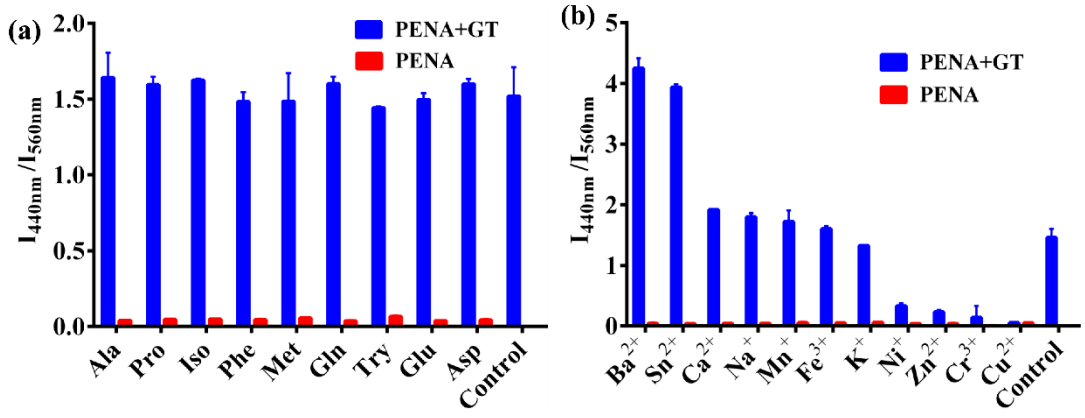

Fig. S8. Interferences of various amino acids (0.5 mM) (a) and metal ions (2 mM) (b) for the glucosylation of **PENA** by GTFs.

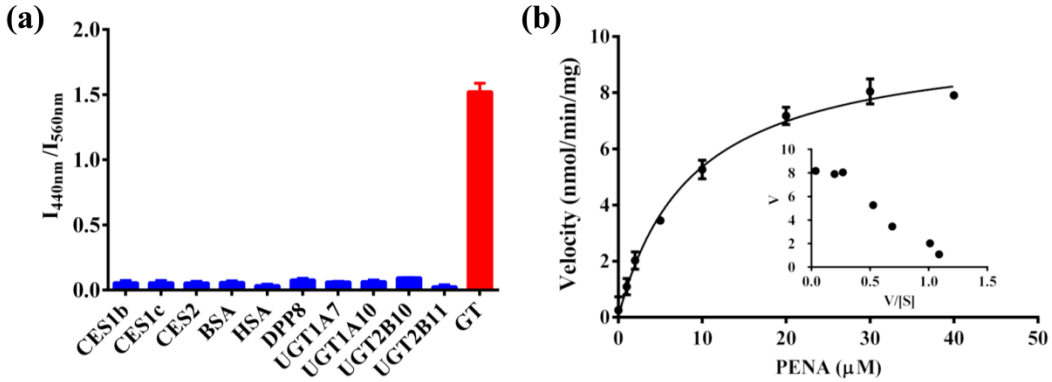

Fig. S9. Enzymatic analysis for glucosylation of **PENA** (5 μM) by GFTs. (a) Specify evaluation for glucosylation of **PENA** mediated by GFTs in comparison with various biological enzymes, including glycosidase glucuronidases (UGT1A7, UGT1A10, UGT2B10, and UGT2B11), hydrolases (CES1b, CES1c, CES2, DPP8), BSA and HSA (10 μg/mL). (b) The kinetics about the glucosylation of **PEN**A by GTFs.

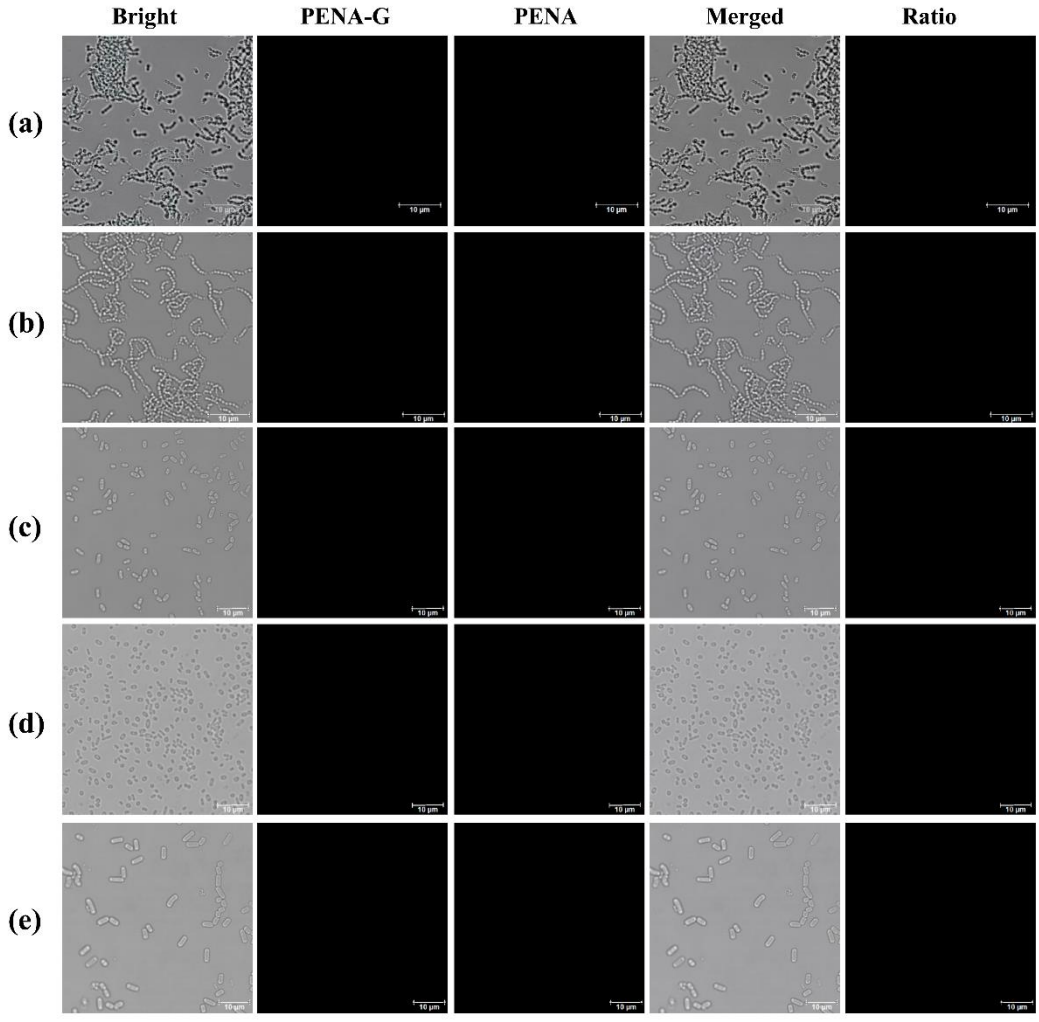

Fig. S10. Fluorescence images of various bacteria blank control groups without

PENA. (a) *Streptococcus mutans*; (b) *Hemolytic streptococcus*; (c) *Lactobacillus amylovorus*; (d) *Streptococcus pasteurianus* strain 080205; (e) *Bacillus cereus* 994000168 LBK.

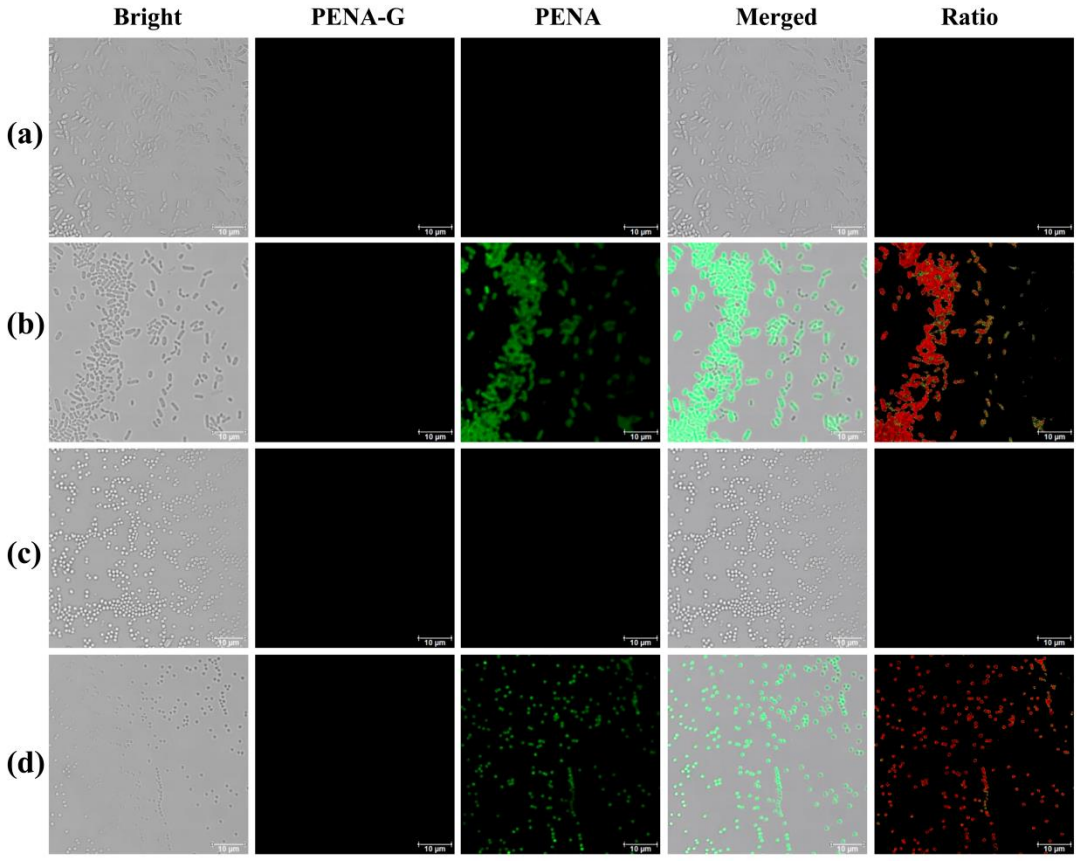

Fig. S11. Fluorescence images of *Escherichia coli* DH5alpha BRL (**a**, blank group without **PENA**; **b**, experimental group with **PENA** 50 μM, Ratio = 0.04); and *Staphylococcus aureus* ssp. aureus DSM 3463 (**c**, blank group without **PENA**; **d**, experimental group with **PENA** 50 μM, Ratio = 0.05).

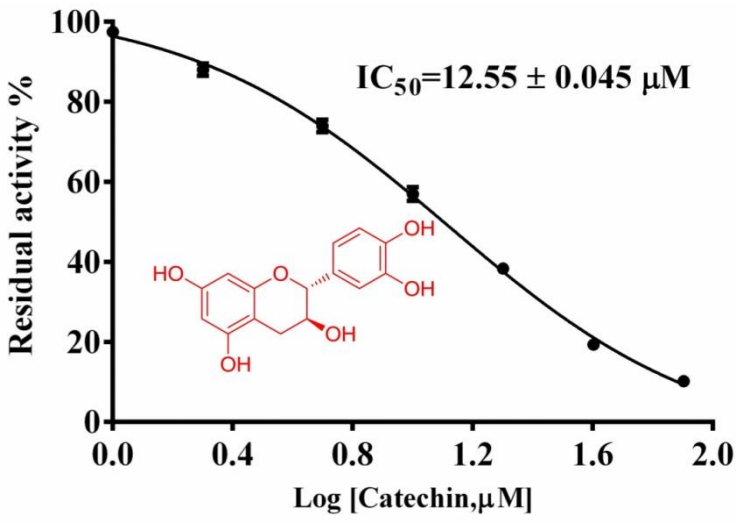

Fig. S12. Dose-dependent inhibitory effect of **CA** on the glucosylation of **PENA** by GTFs.

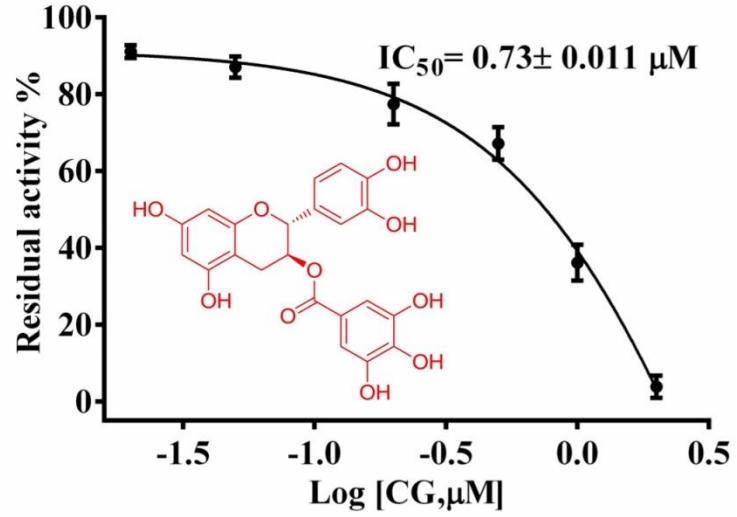

Fig. S13. Dose-dependent inhibitory effect of **CG** on the glucosylation of **PENA** by GTFs.

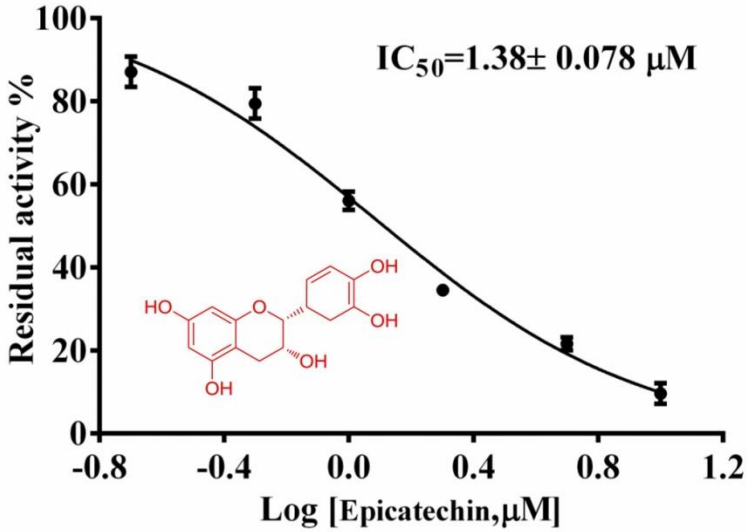

Fig. S14. Dose-dependent inhibitory effect of **ECA** on the glucosylation of **PENA** by GTFs.

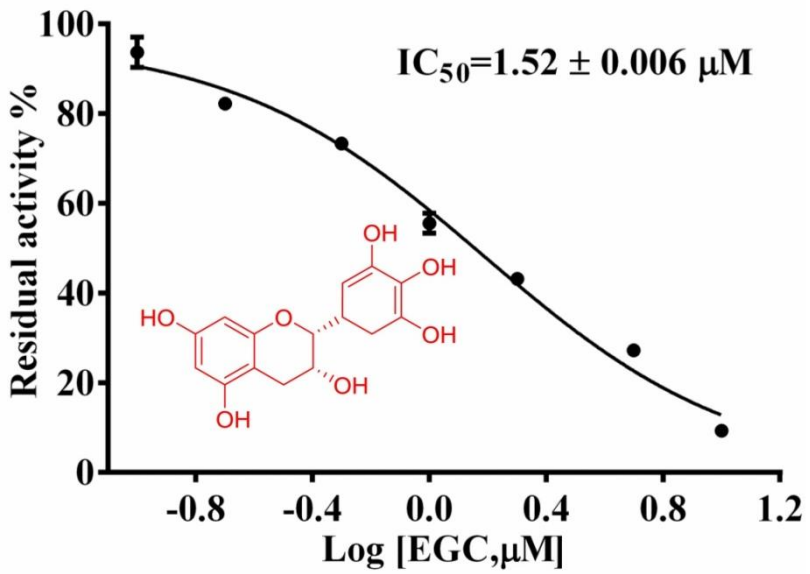

Fig. S15. Dose-dependent inhibitory effect of **EGC** on the glucosylation of **PENA** by GTFs.

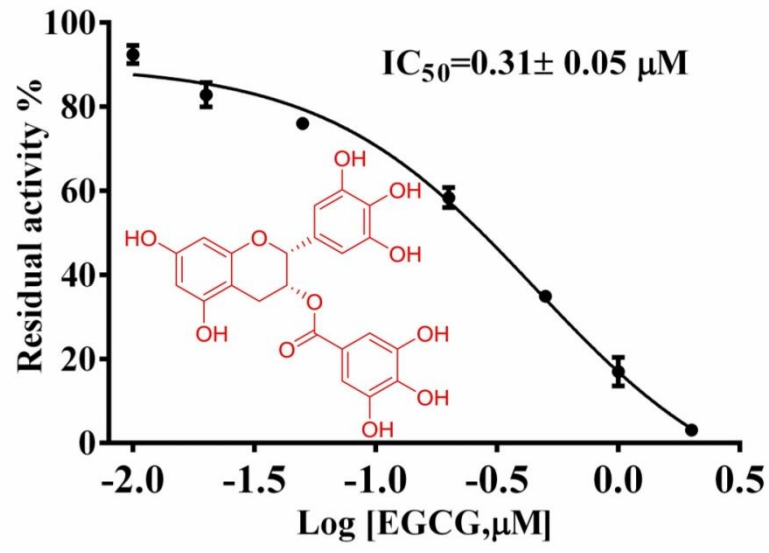

Fig. S16. Dose-dependent inhibitory effect of **EGCG** on the glucosylation of **PENA** by GTFs.

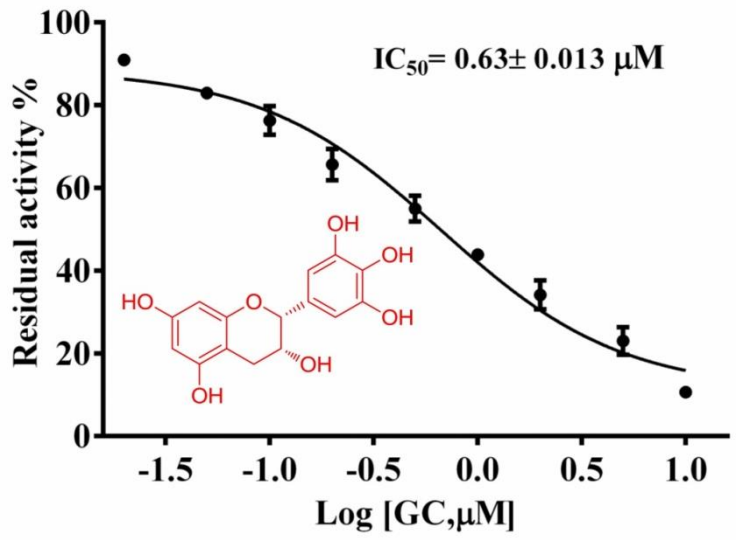

Fig. S17. Dose-dependent inhibitory effect of **GC** on the glucosylation of **PENA** by GTFs.

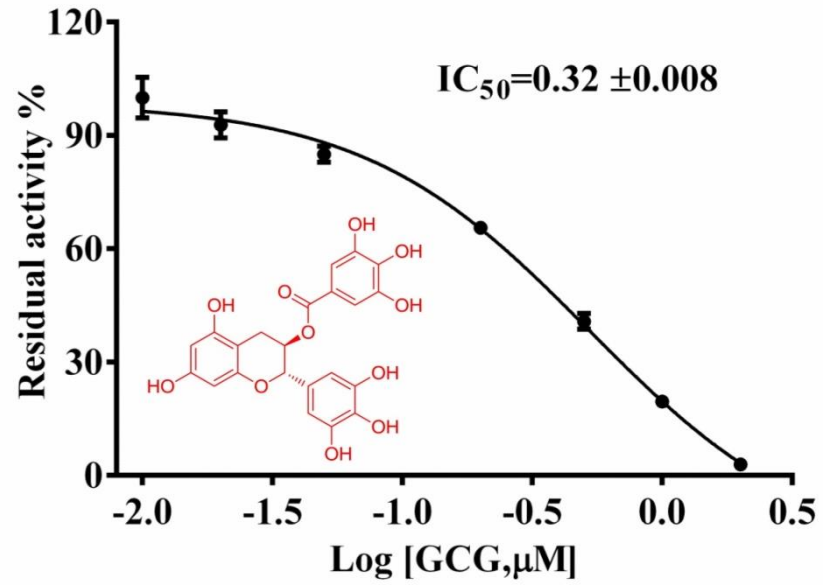

Fig. S18. Dose-dependent inhibitory effect of **GCG** on the glucosylation of **PENA** by GTFs.

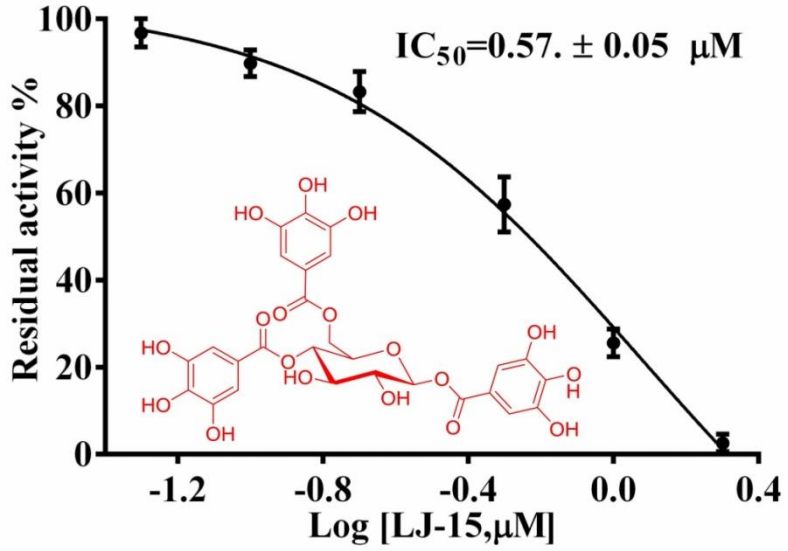

Fig. S19. Dose-dependent inhibitory effect of **TGG** on the glucosylation of **PENA** by GTFs.

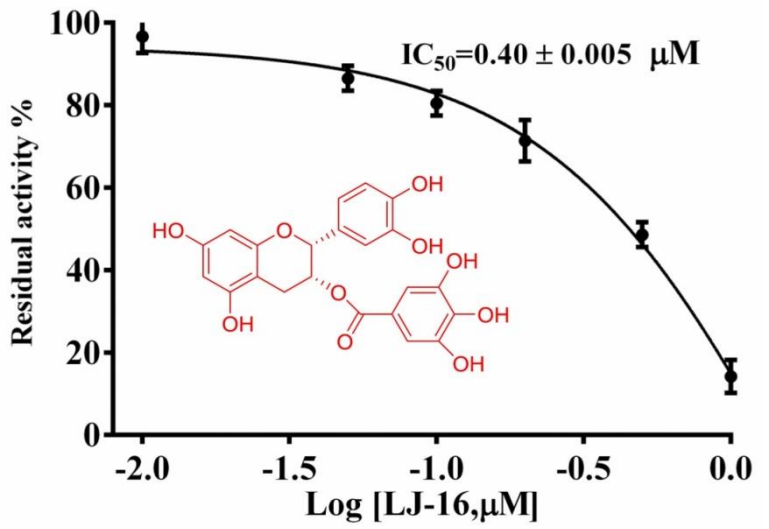

Fig. S20. Dose-dependent inhibitory effect of **ECG** on the glucosylation of **PENA** by GTFs.

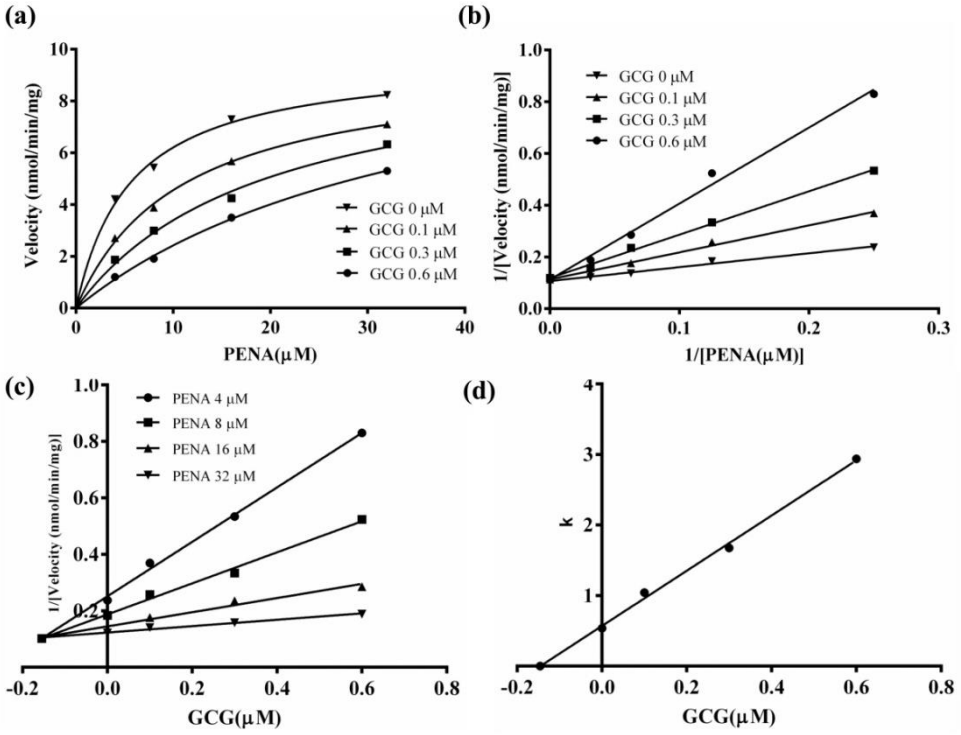

Fig. S21. Inhibition kinetics of **GCG** on the glucsoylation of **PENA** mediated by GTFs. (a,b) Lineweaver–Burk plot of **GCG**'s inhibition towards the activity of GTFs; (c) Dixon plot of **GCG**'s inhibition towards the activity of GTFs; (d) determination of inhibition kinetic parameter (Ki) using the slopes from Lineweaver–Burk plot towards the concentration of **GCG**. The data points represent the mean value of duplicateexperiments.

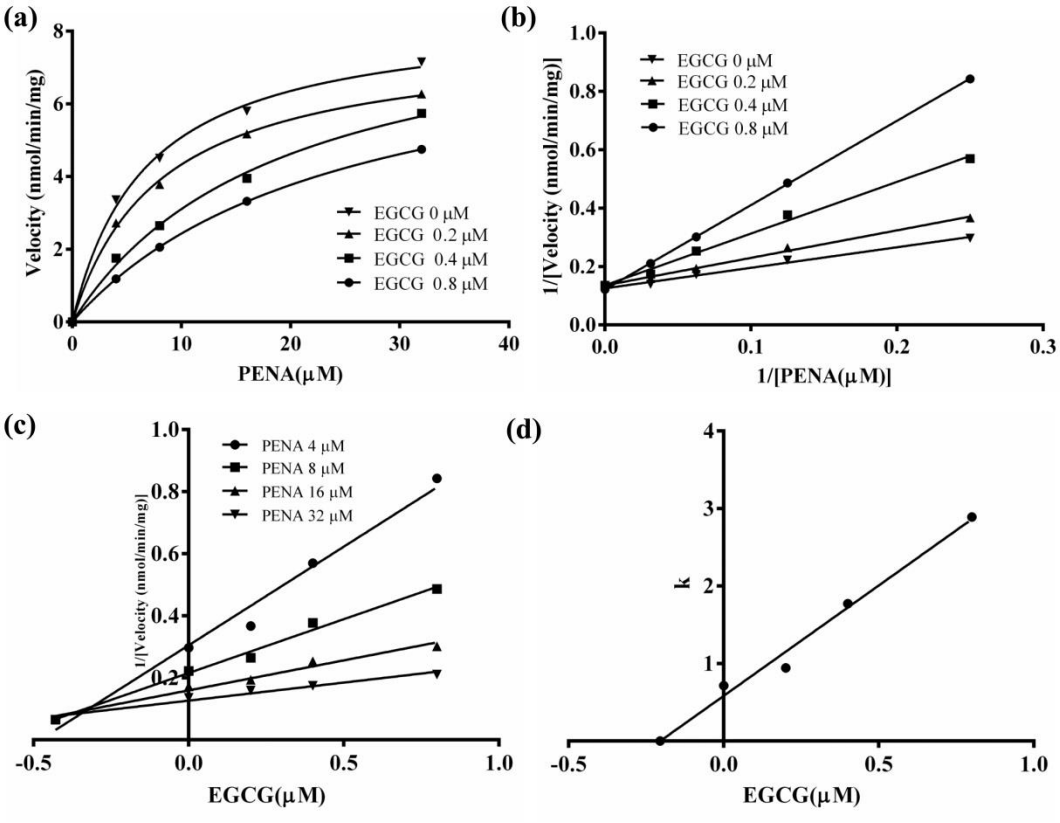

Fig. S22. Inhibition kinetics of **EGCG** on the glucsoylation of **PENA** mediated by GTFs. (a,b) Lineweaver–Burk plot of **EGCG**'s inhibition towards the activity of GTFs; (c) Dixon plot of **EGCG**'s inhibition towards the activity of GTFs; (d) determination of inhibition kinetic parameter (Ki) using the slopes from Lineweaver–Burk plot towards the concentration of **EGCG**. The data points represent the mean value of duplicate experiments.

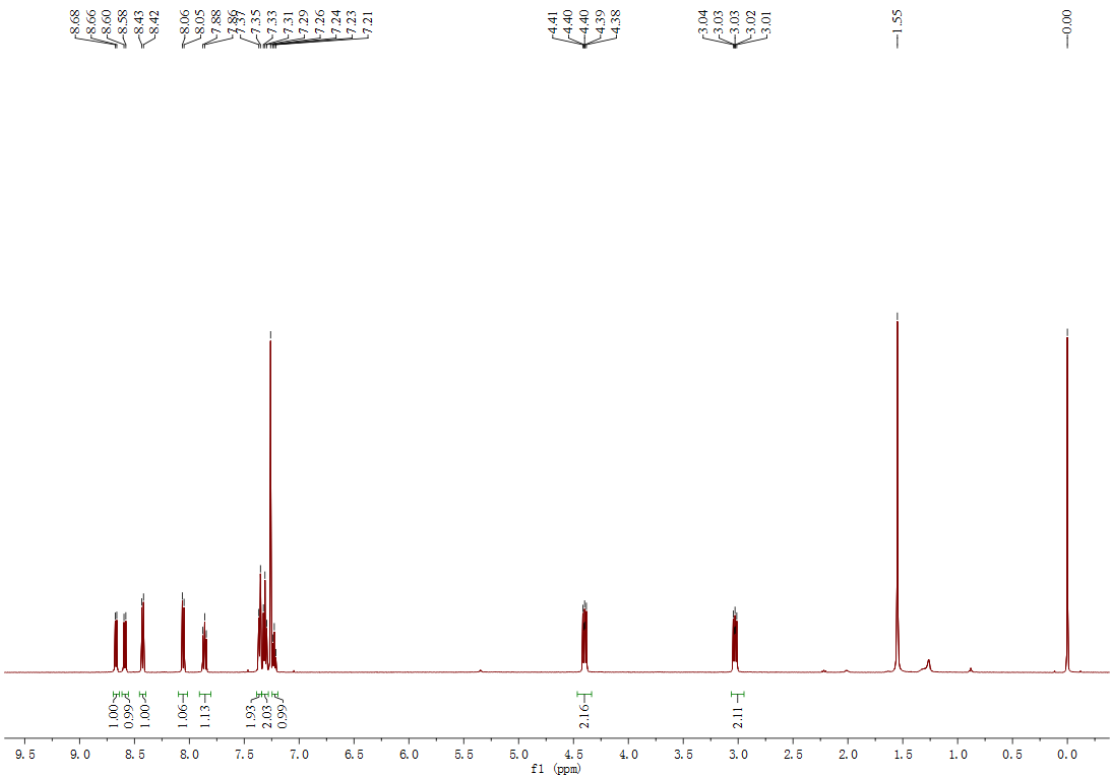

Fig. S23. ^{1}H NMR spectrum of compound **1**.

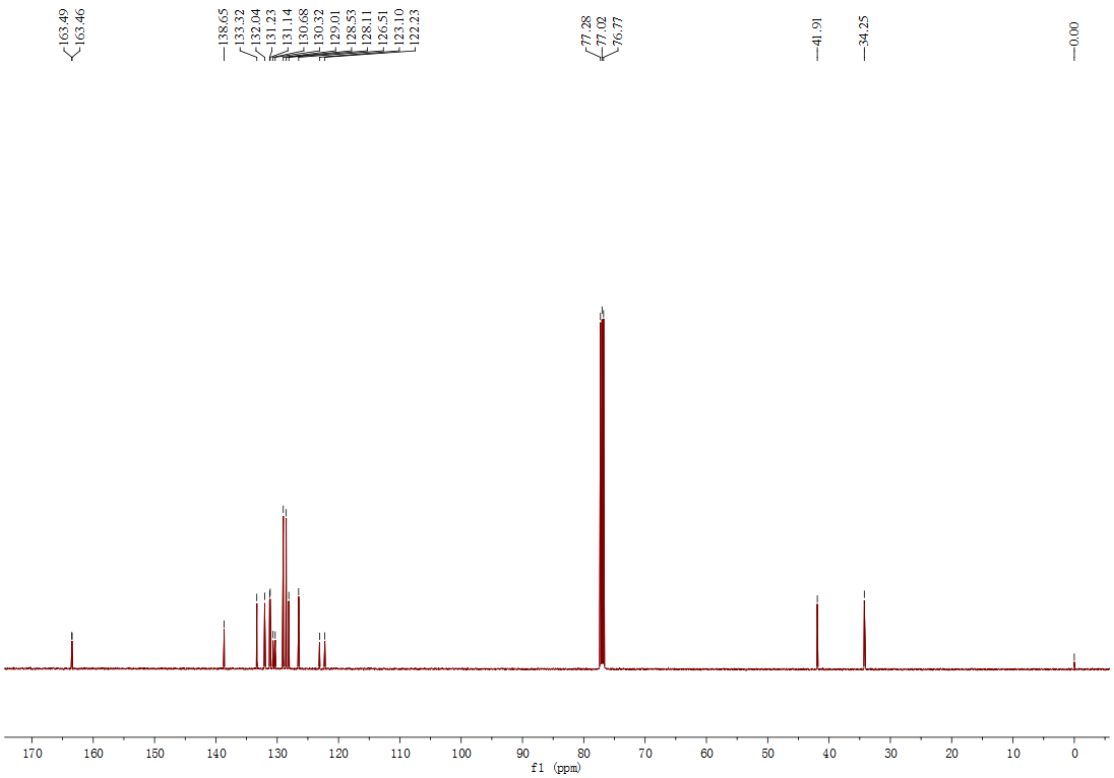

Fig. S24. ^{13}C NMR spectrum of compound **1**

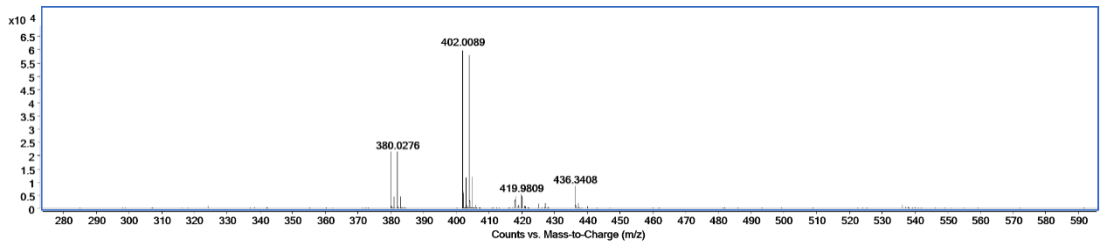

Fig. S25. HR-MS of compound **1**

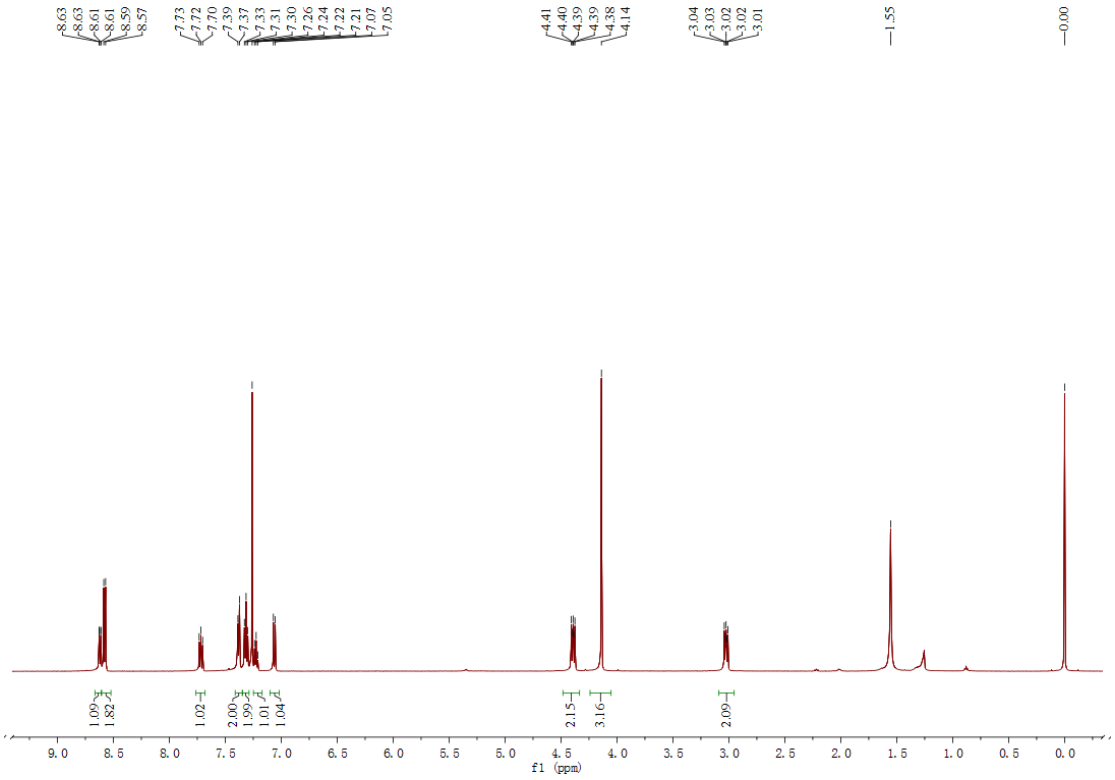

Fig. S26. ^{1}H NMR spectrum of compound **2**

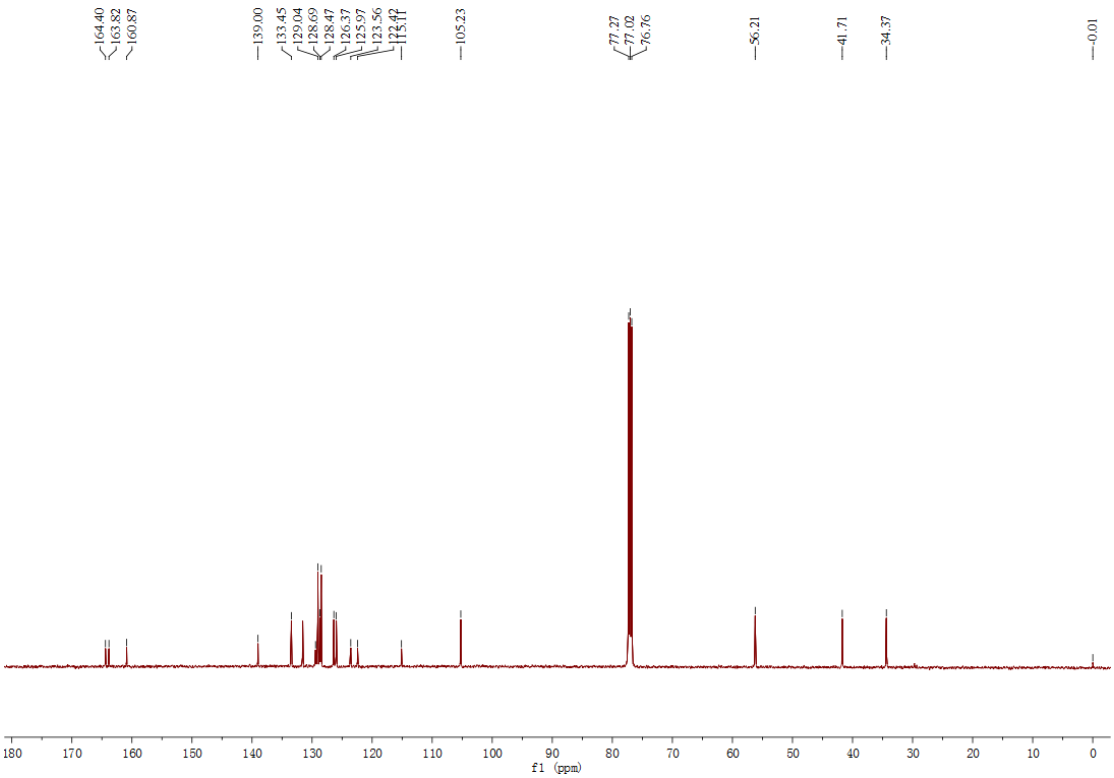

Fig. S27. ^{13}C NMR spectrum of compound **2**

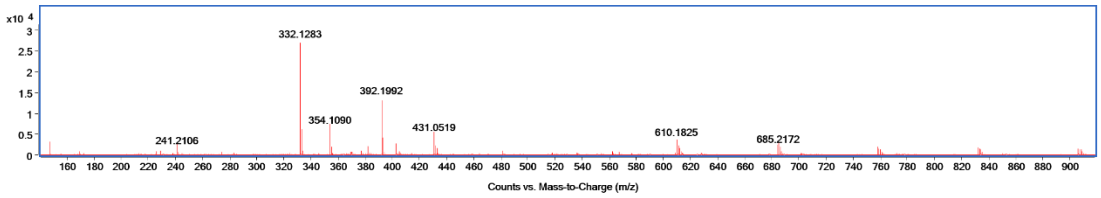

Fig. S28. HR-MS of compound **2**

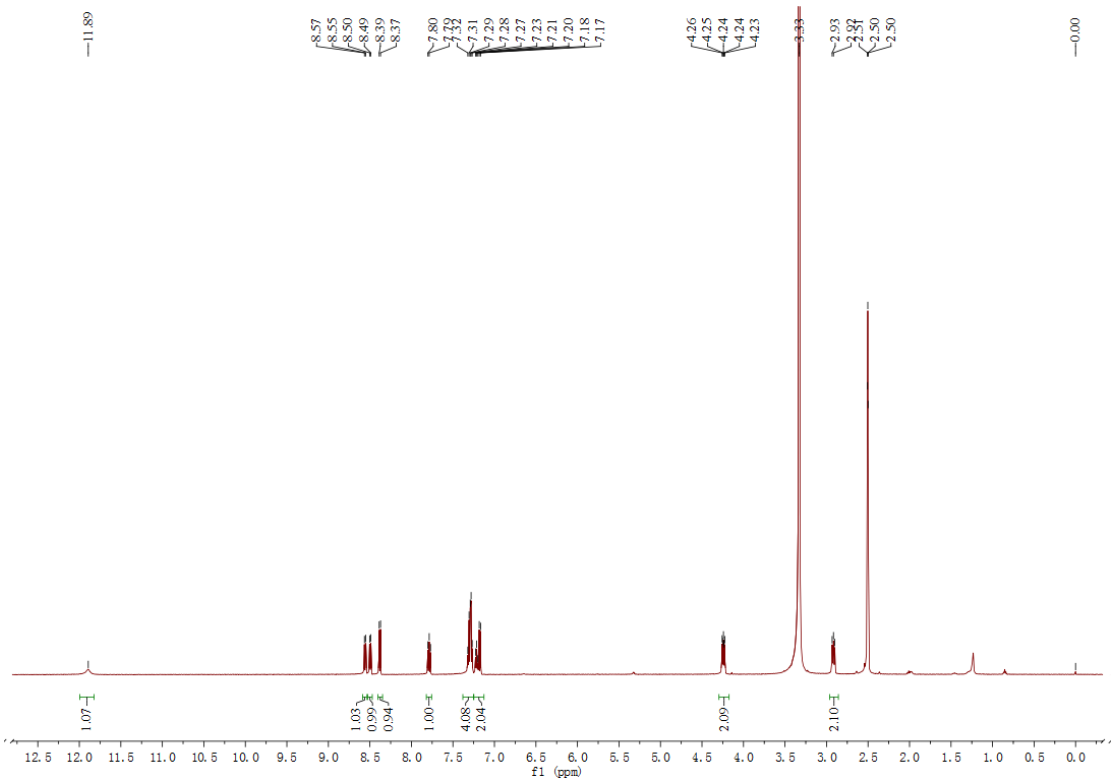

Fig. S29. ^{1}H NMR spectrum of **PENA**

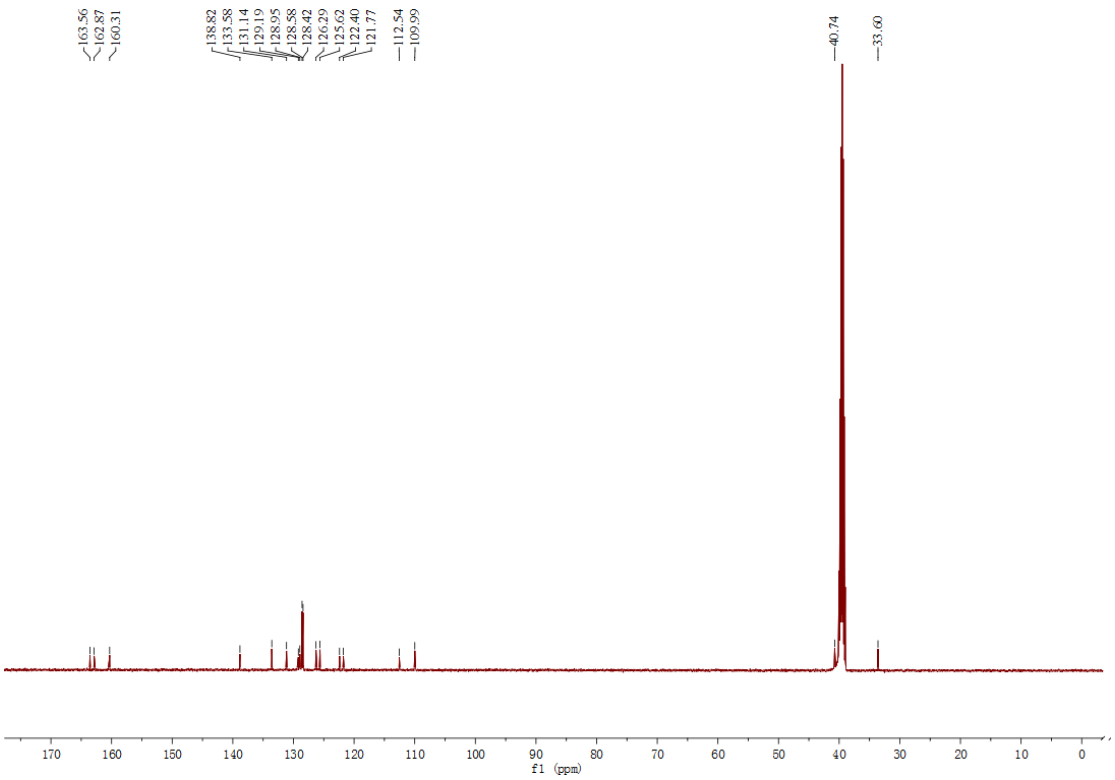

Fig. S30. ^{13}C NMR spectrum of **PENA**

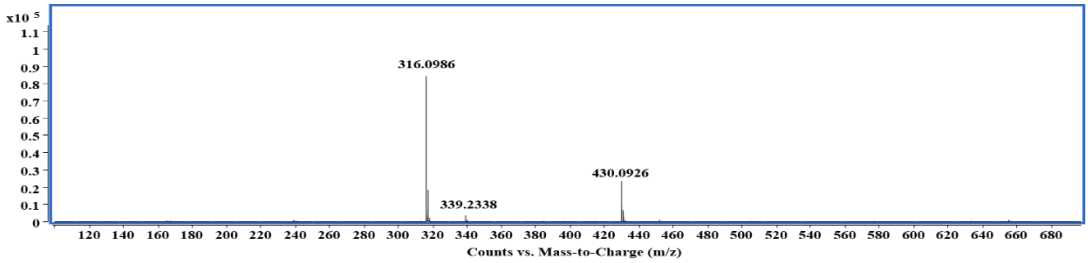

Fig. S31. HR-MS of **PENA**

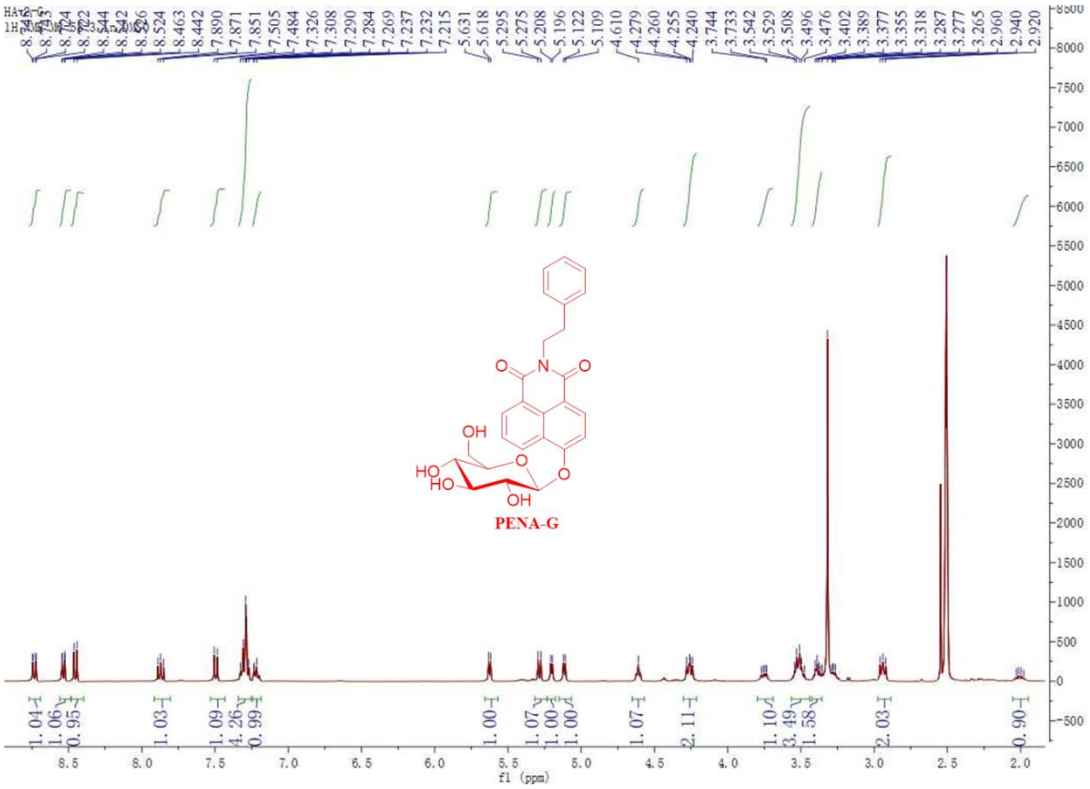

Fig. S32. ^{1}H NMR spectrum of **PENA-G**

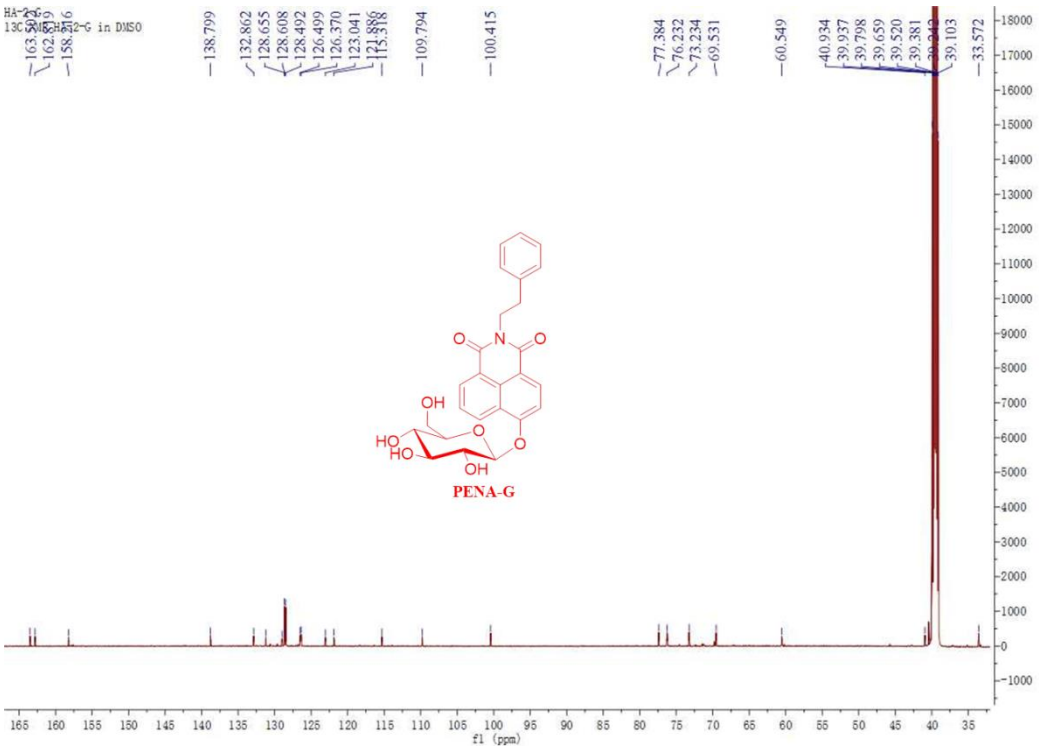

Fig. S33. ^{13}C NMR spectrum of **PENA-G**

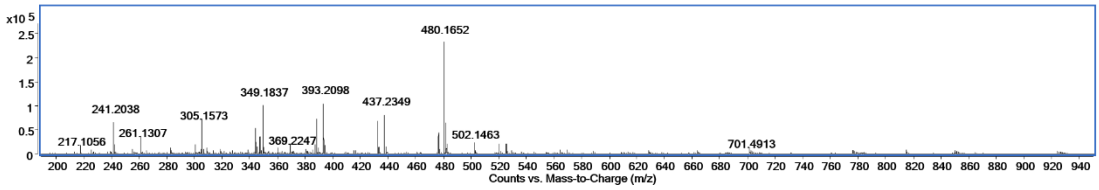

Fig. S34. HR-MS of **PENA-G**

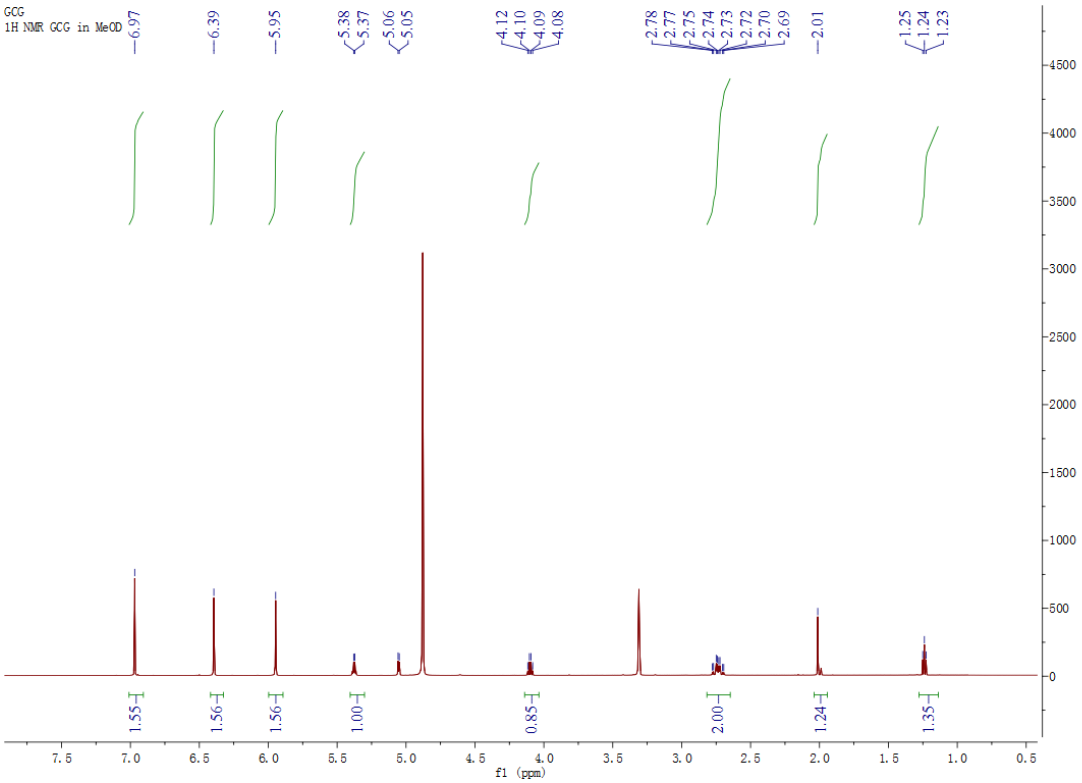

Fig. S35. ^{1}H-NMR spectrum of **GCG**.

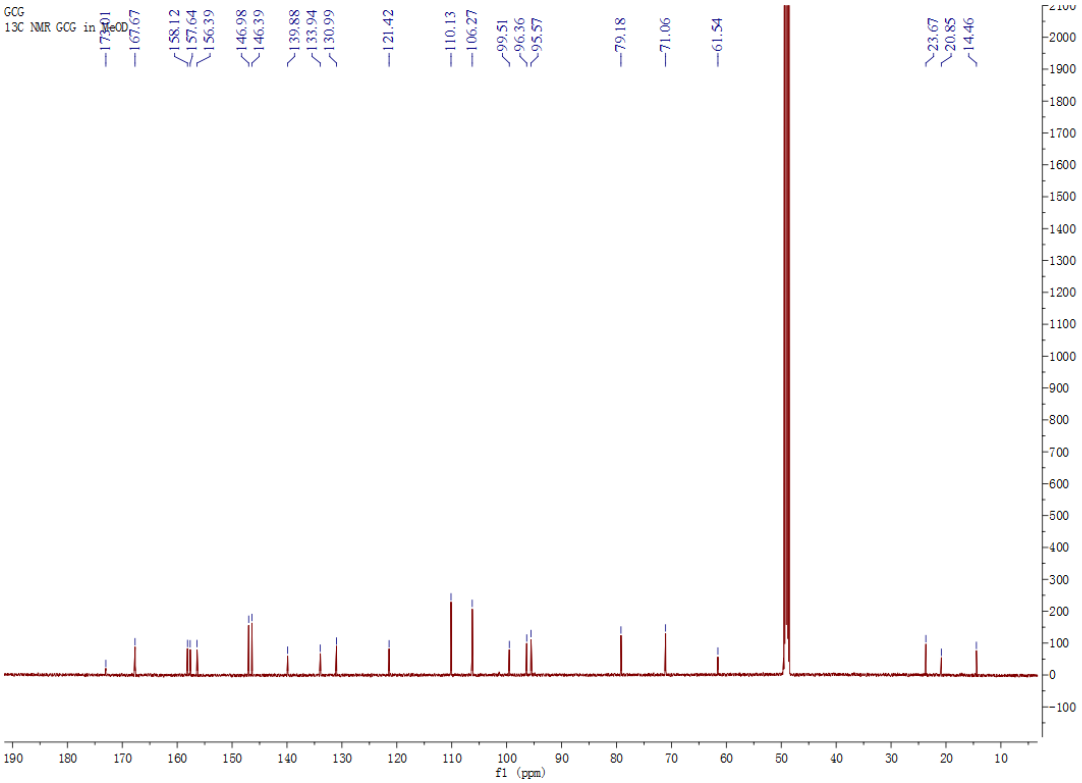

Fig. S36. ^{13}C-NMR spectrum of **GCG**.

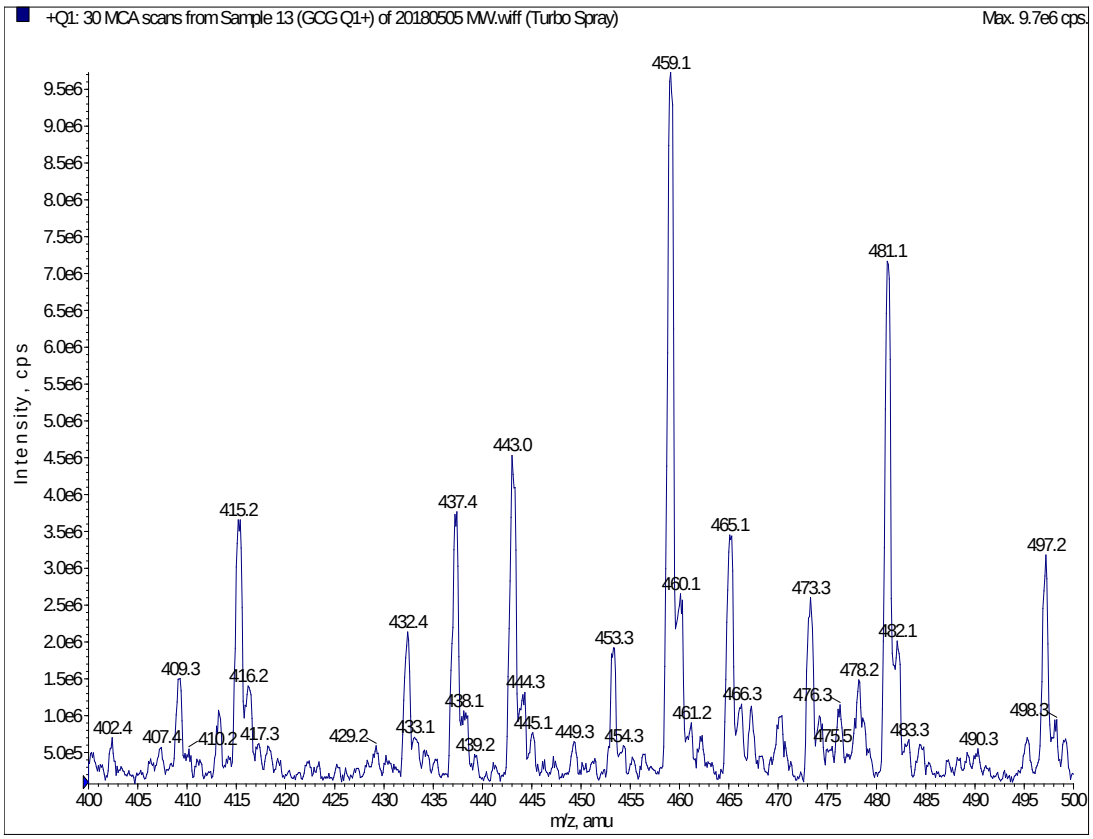

Fig. S37. (+)-ESI-MS spectrum of **GCG**.

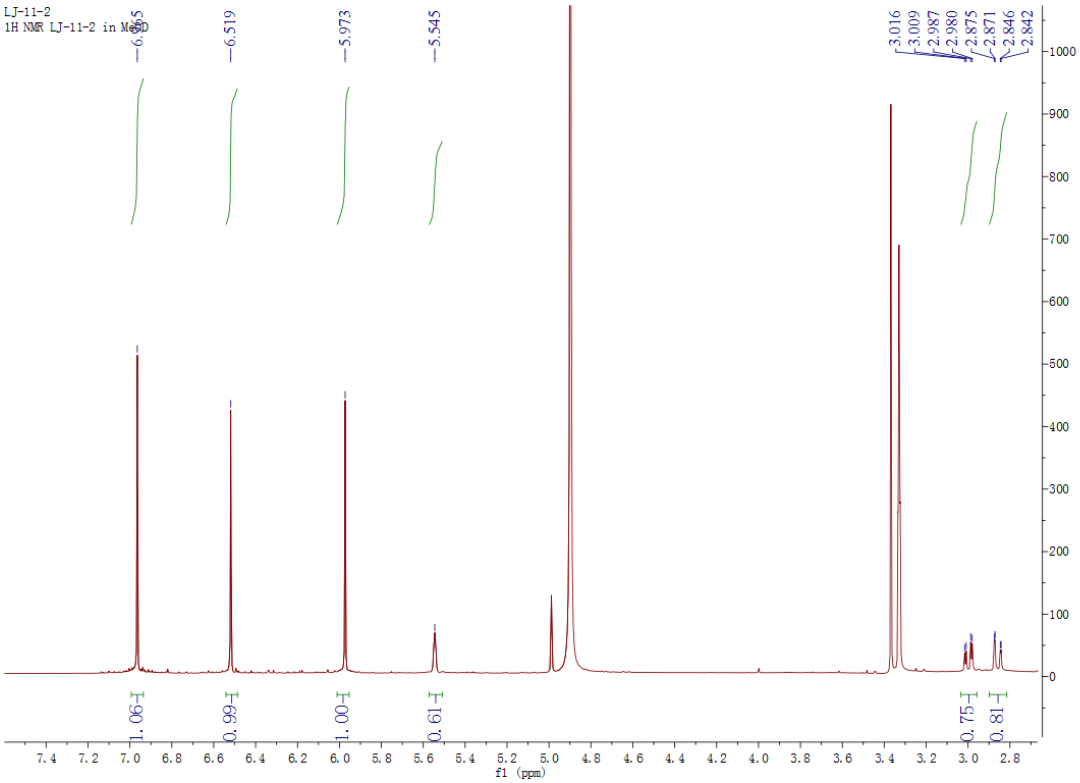

Fig. S38. ^{1}H-NMR spectrum of **EGCG**.

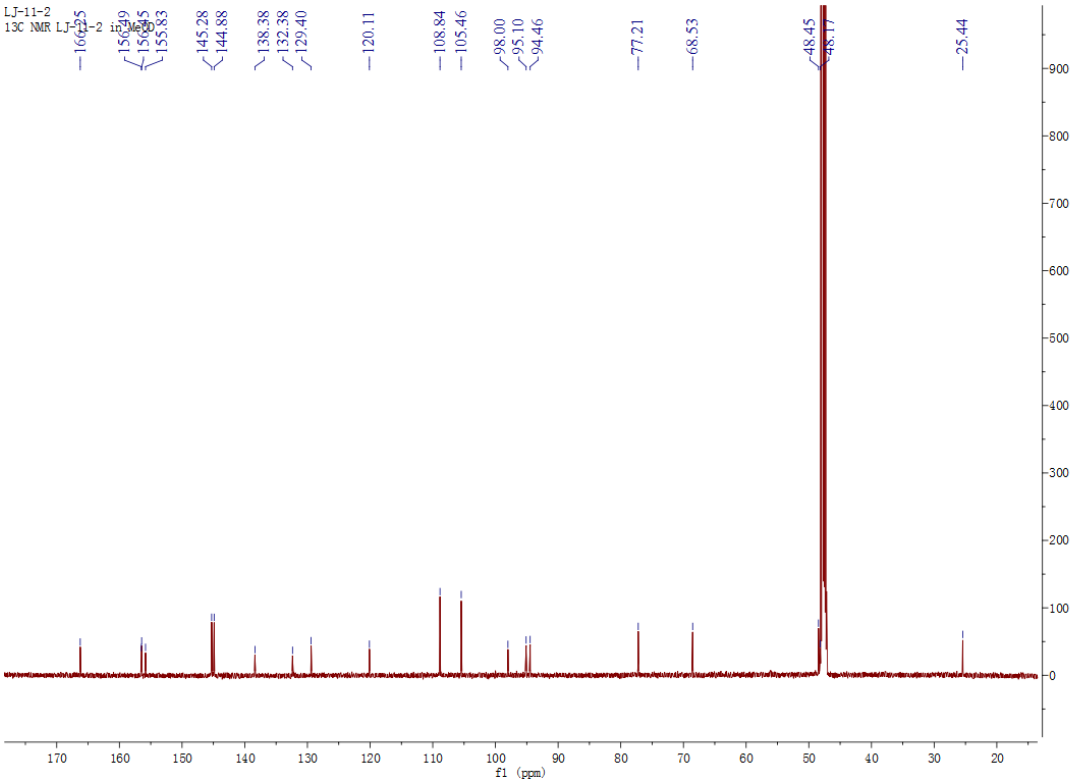

Fig. S39. ^{13}C-NMR spectrum of **EGCG**.

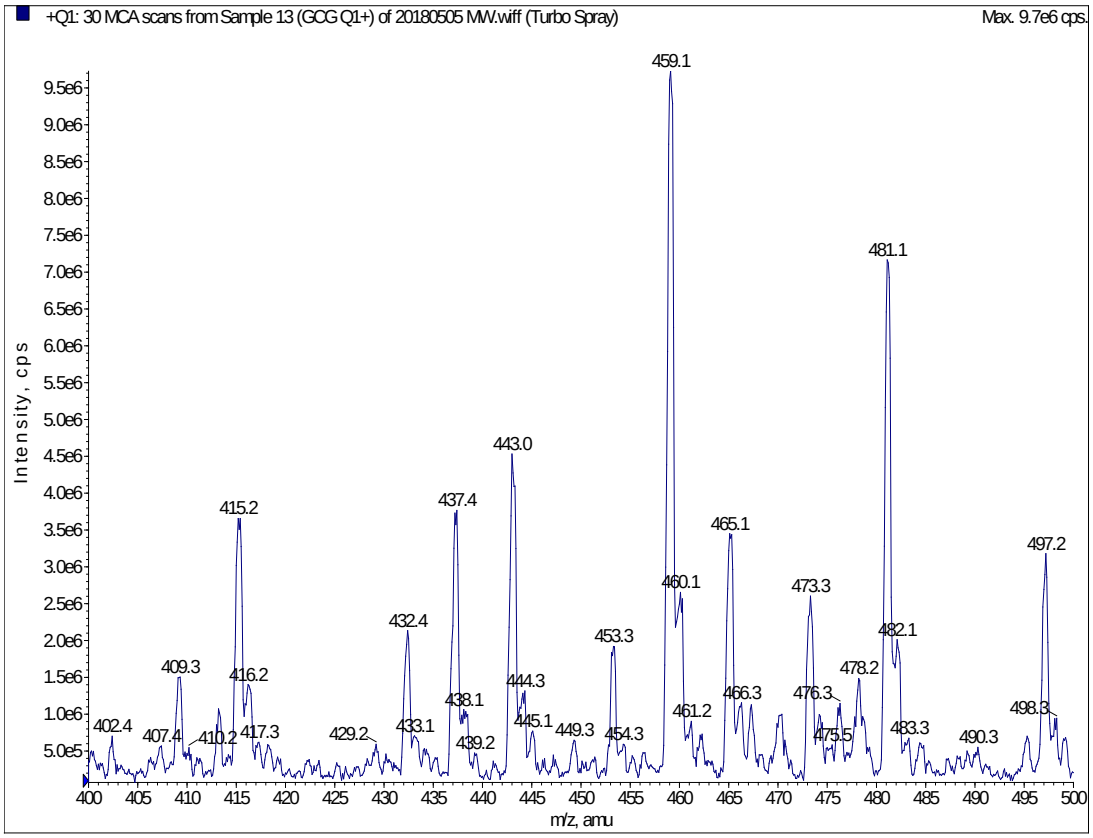

Fig. S40. (+)-ESI-MS spectrum of **EGCG**.

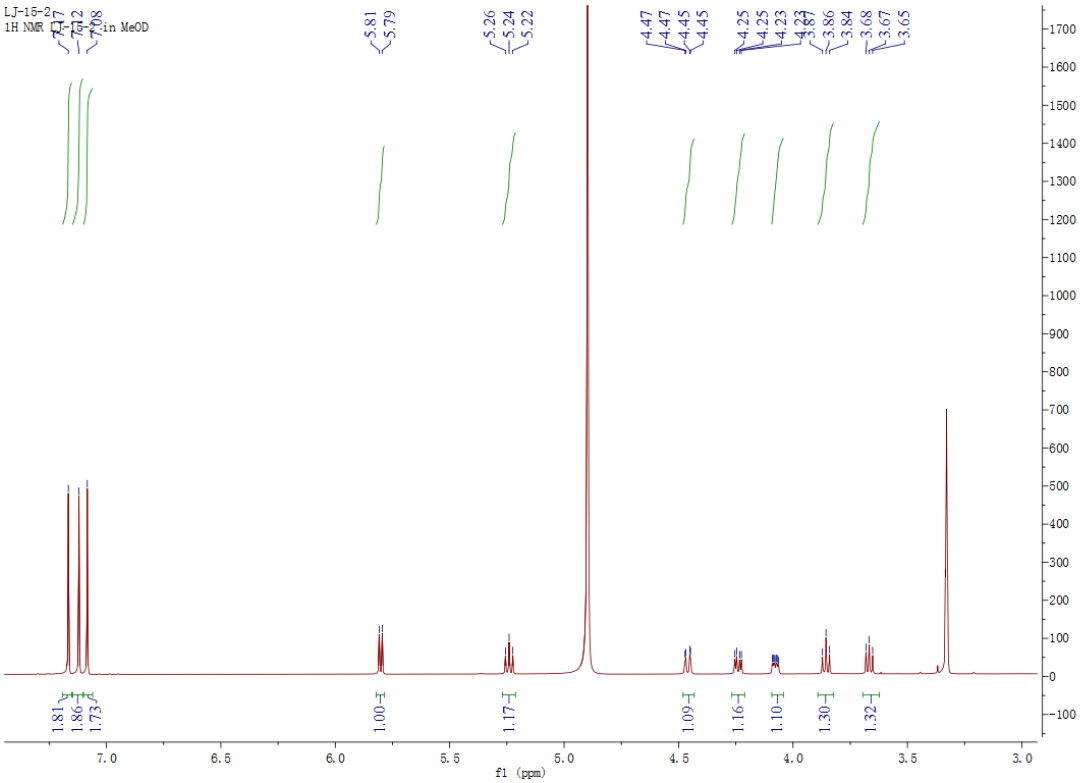

Fig. S41. ^{1}H-NMR spectrum of **TGG**.

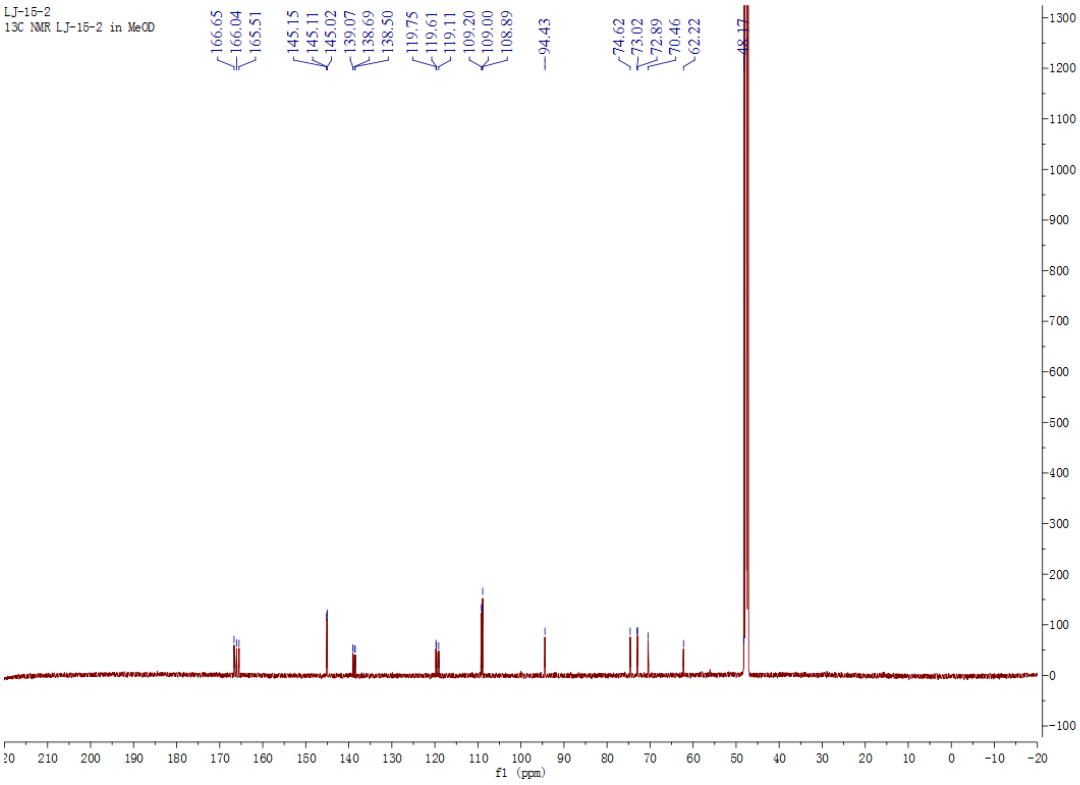

Fig. S42. ^{13}C-NMR spectrum of **TGG**.

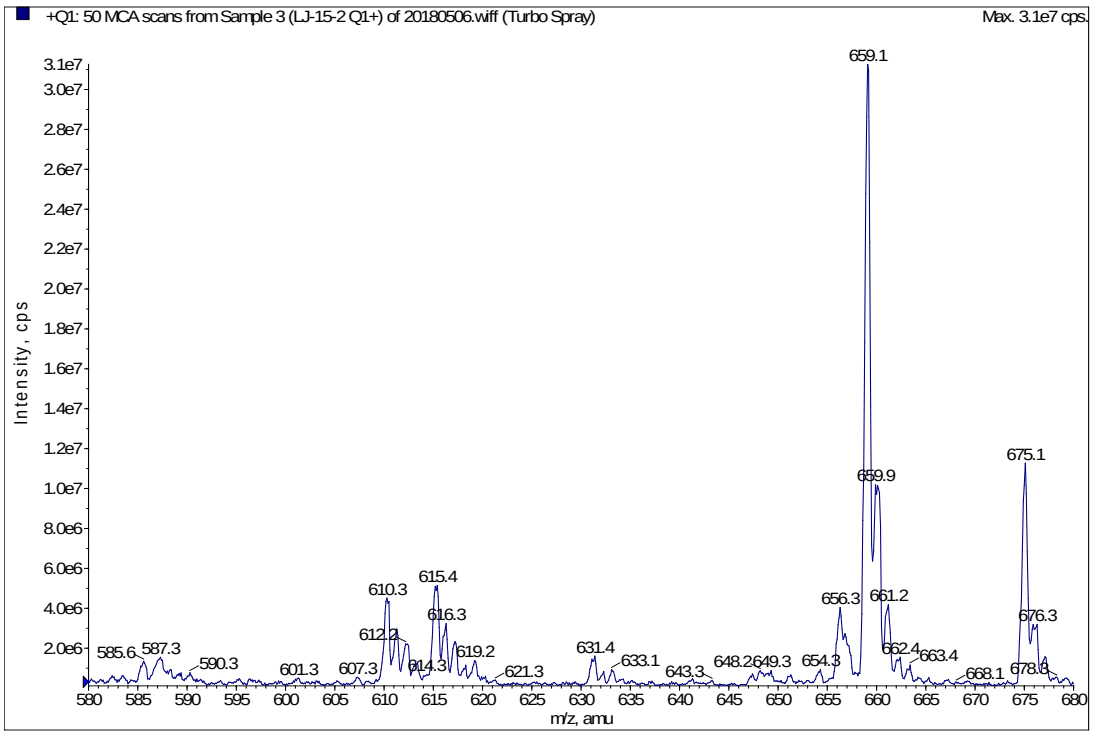

Fig. S43. (+)-ESI-MS spectrum of **TGG**.

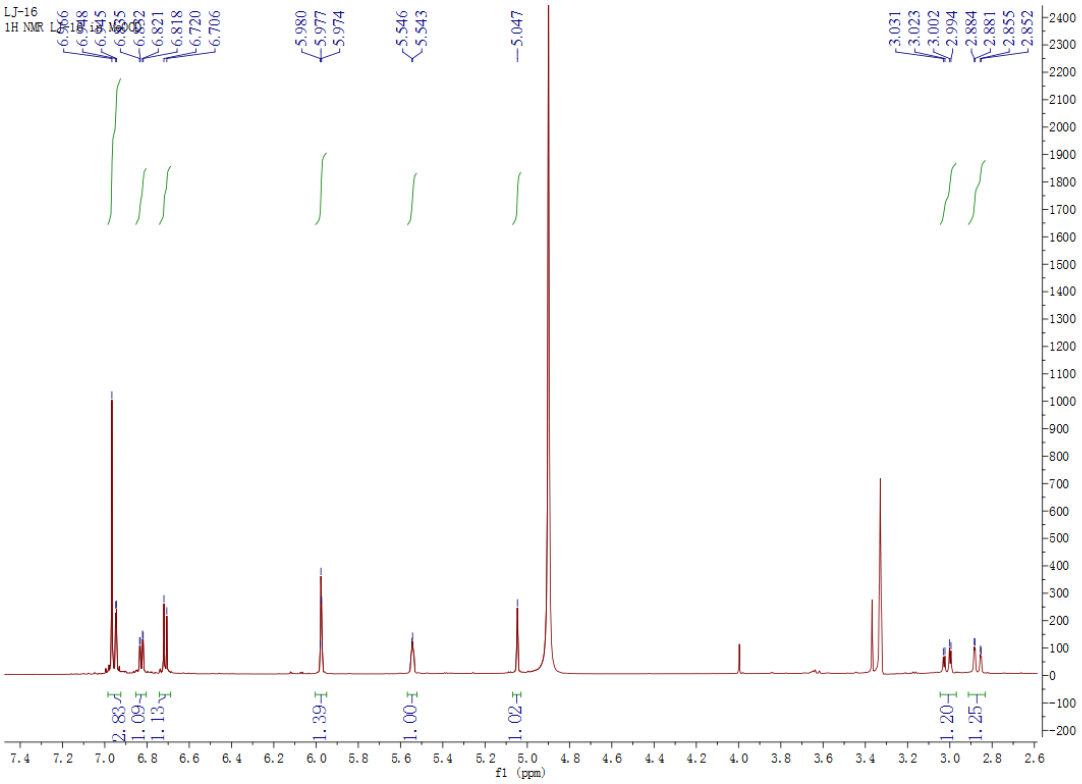

Fig. S44. ^{1}H-NMR spectrum of **ECG**.

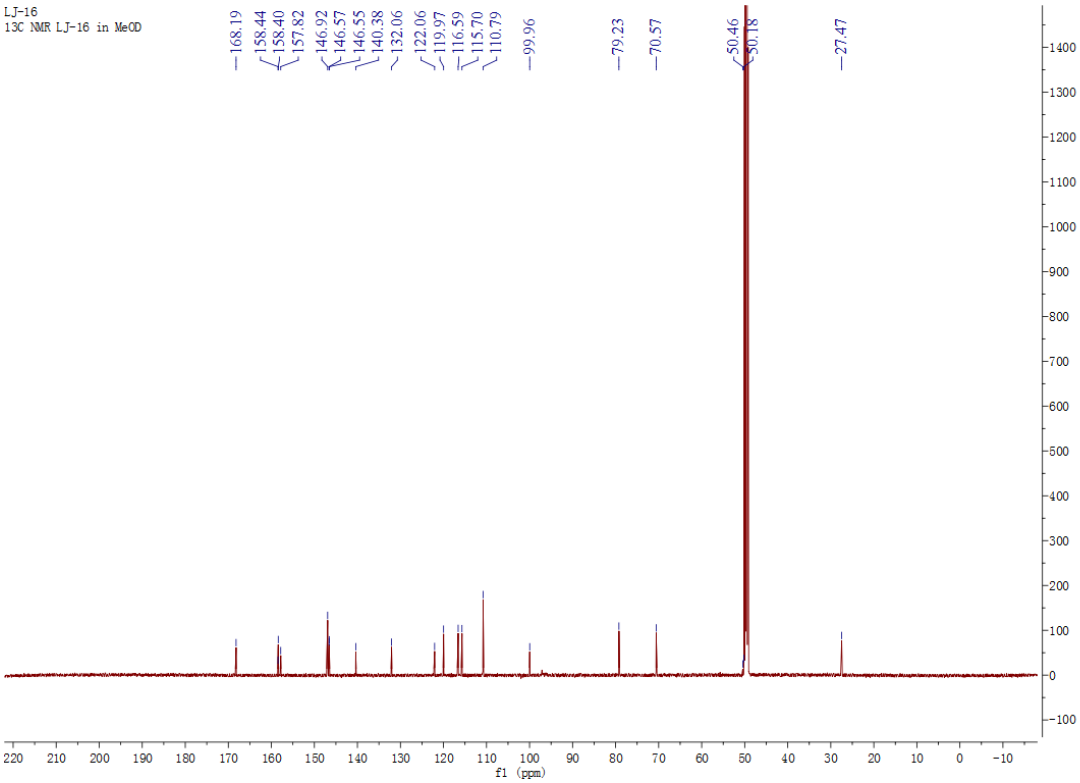

Fig. S45. ^{13}C-NMR spectrum of **ECG**.

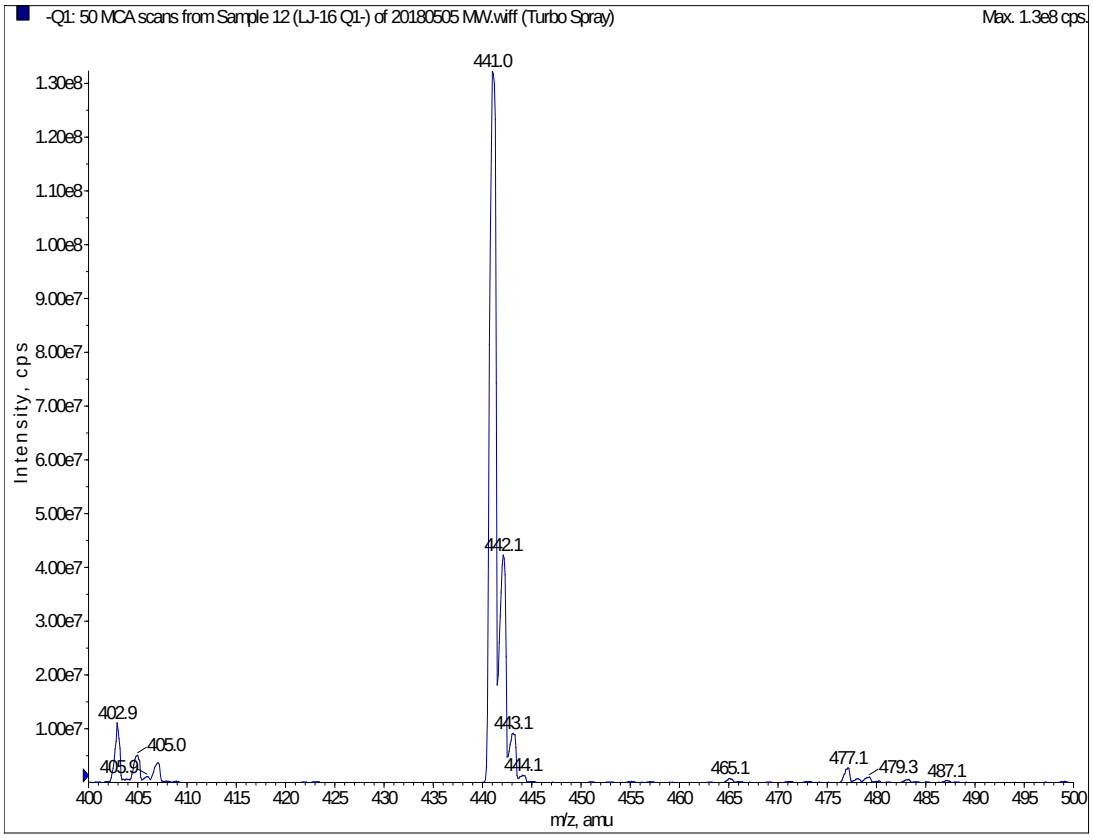

Fig. S46. (-)-ESI-MS spectrum of **ECG**.

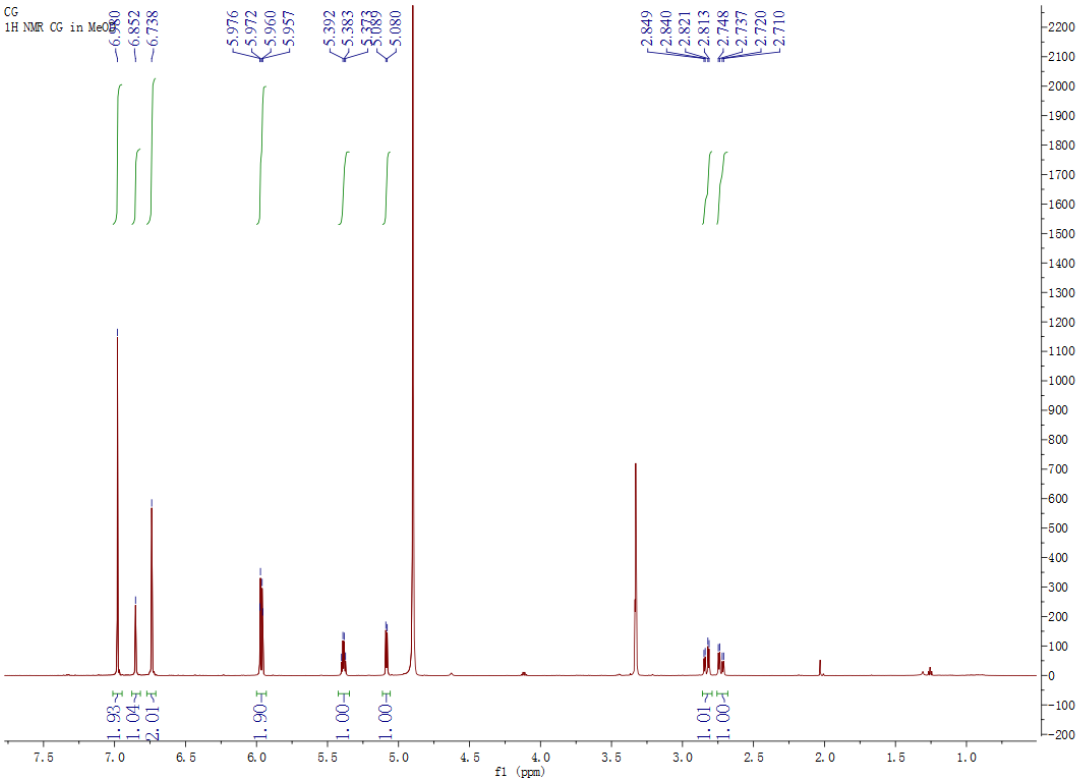

Fig. S47. ^{1}H-NMR spectrum of **CG**.

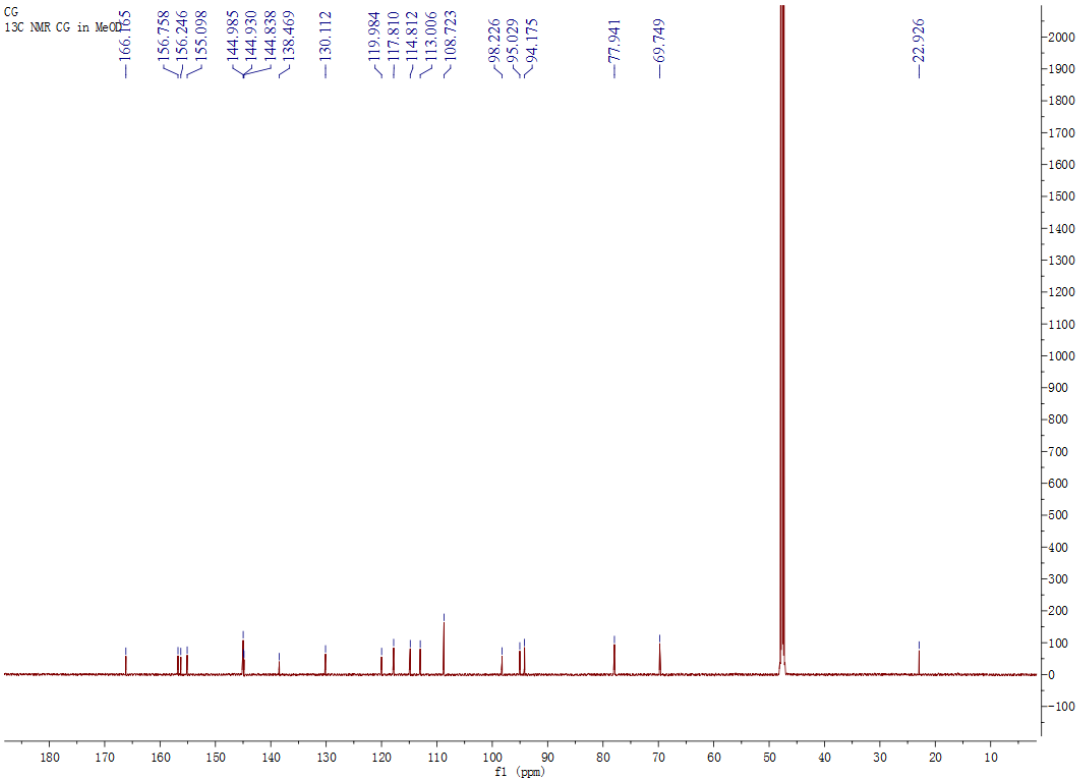

Fig. S48. ^{13}C-NMR spectrum of **CG**.

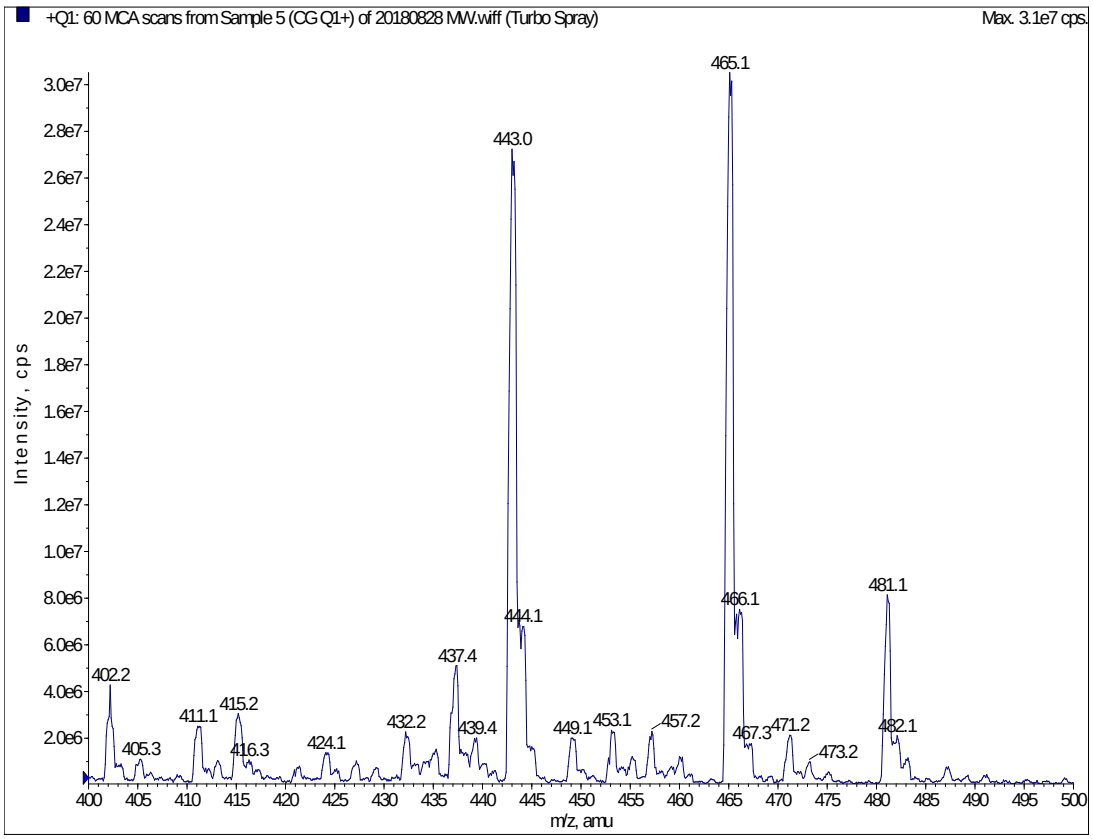

Fig. S49. (+)-ESI-MS of **CG**.

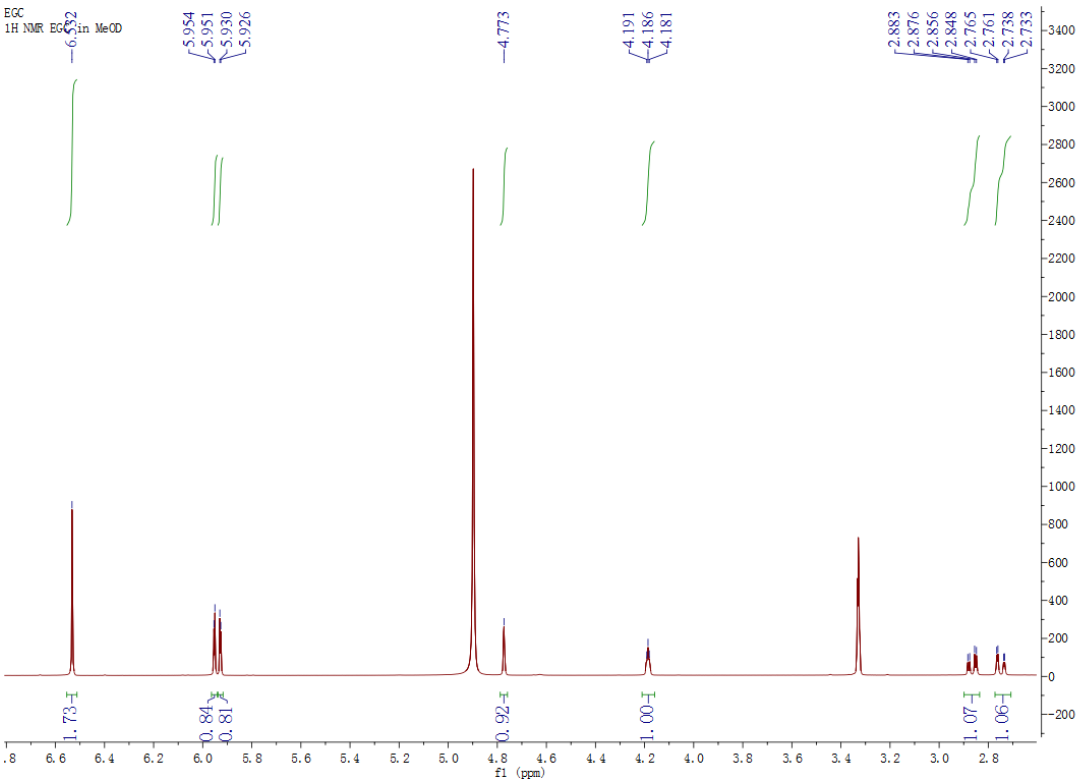

Fig. S50. ^{1}H-NMR spectrum of **EGC**.

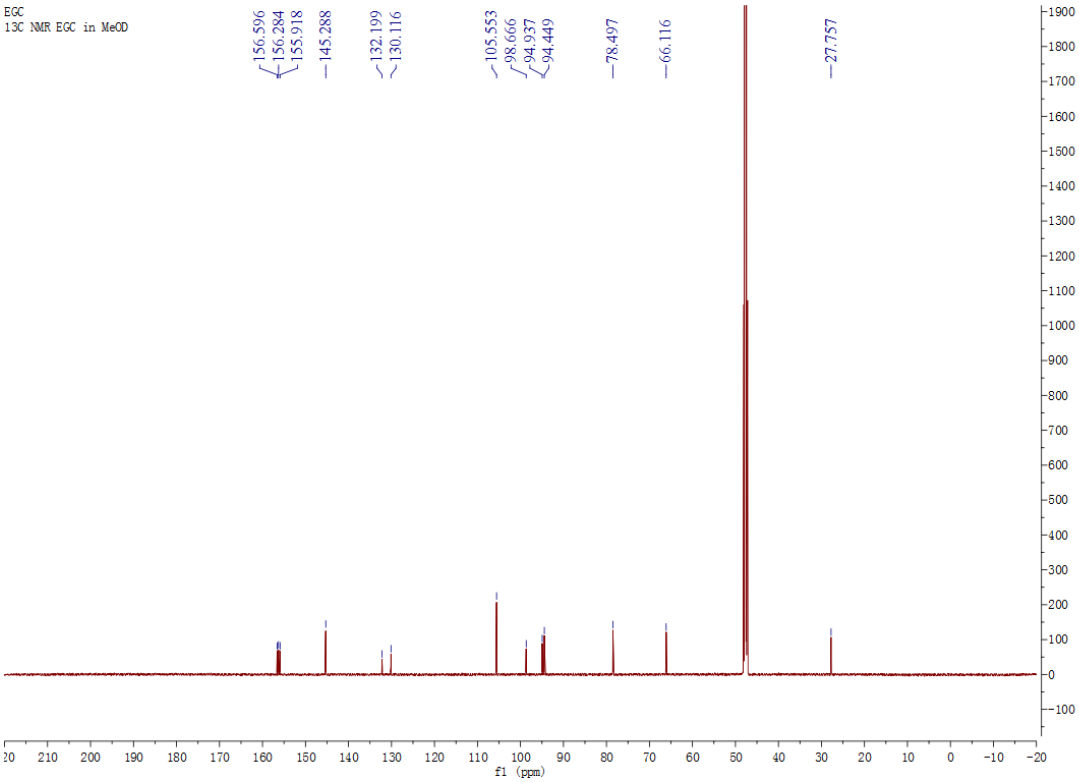

Fig. S51. ^{13}C-NMR spectrum of **EGC**.

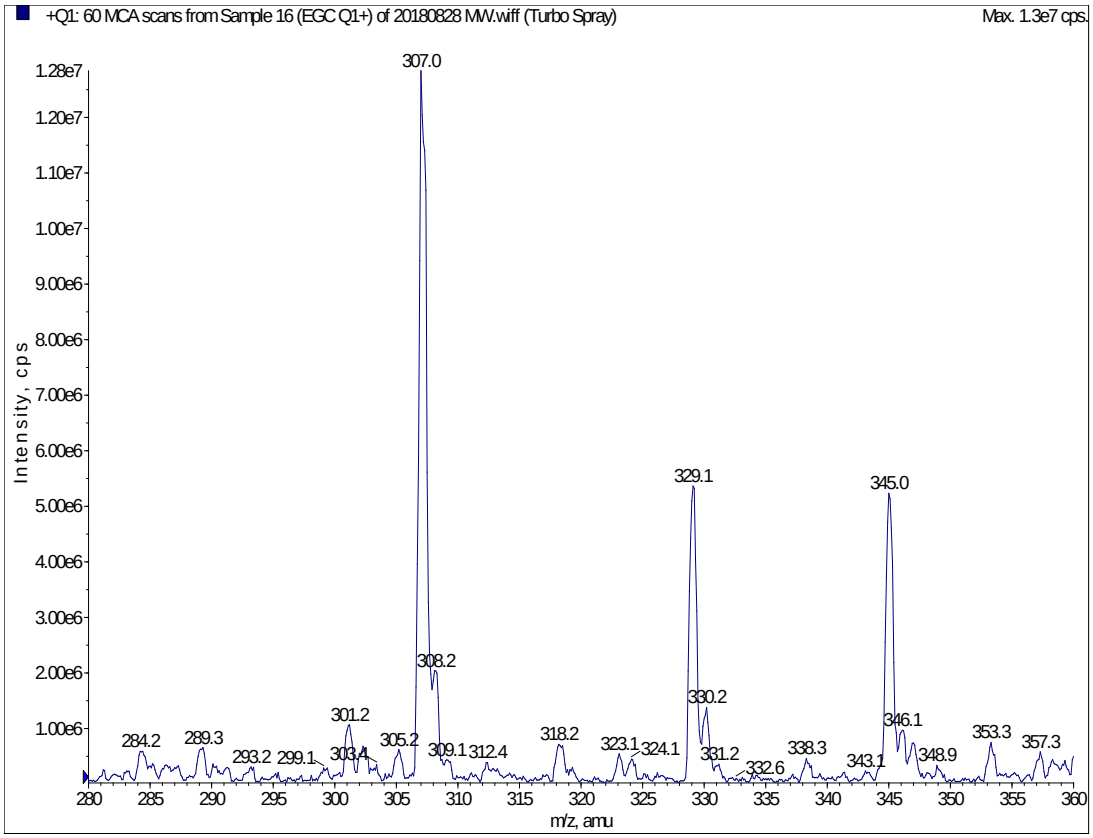

Fig. S52. (+)-ESI-MS of **EGC**.

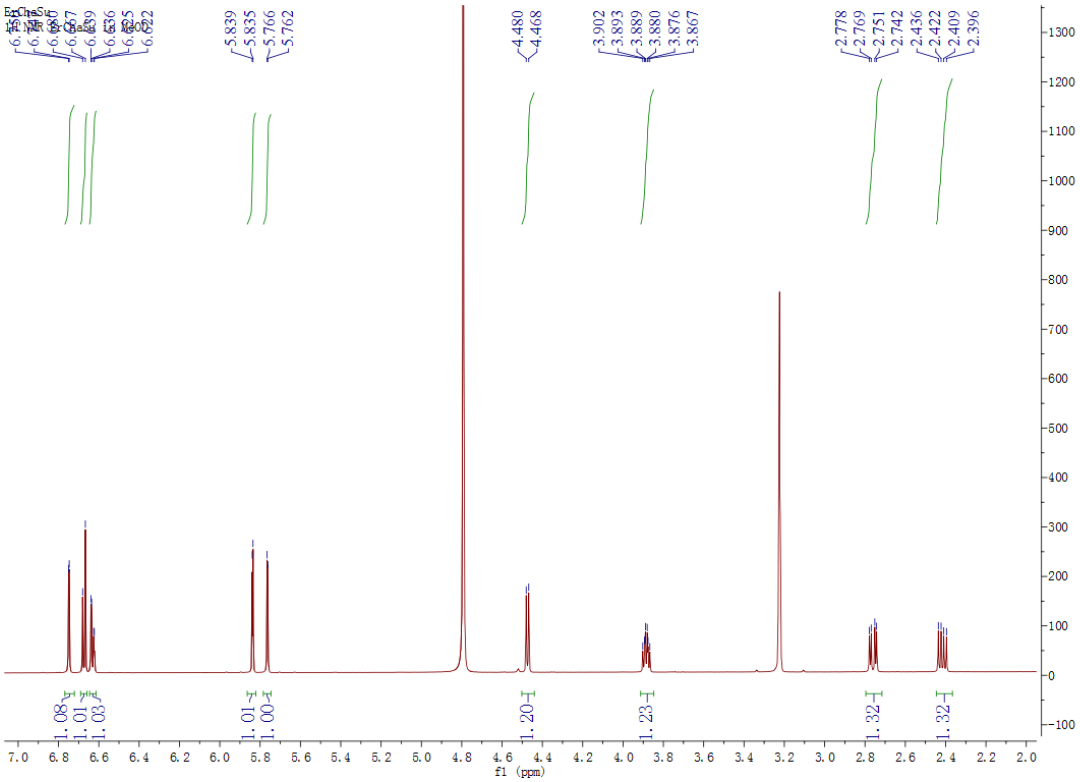

Fig. S53. ^{1}H-NMR spectrum of **CA**.

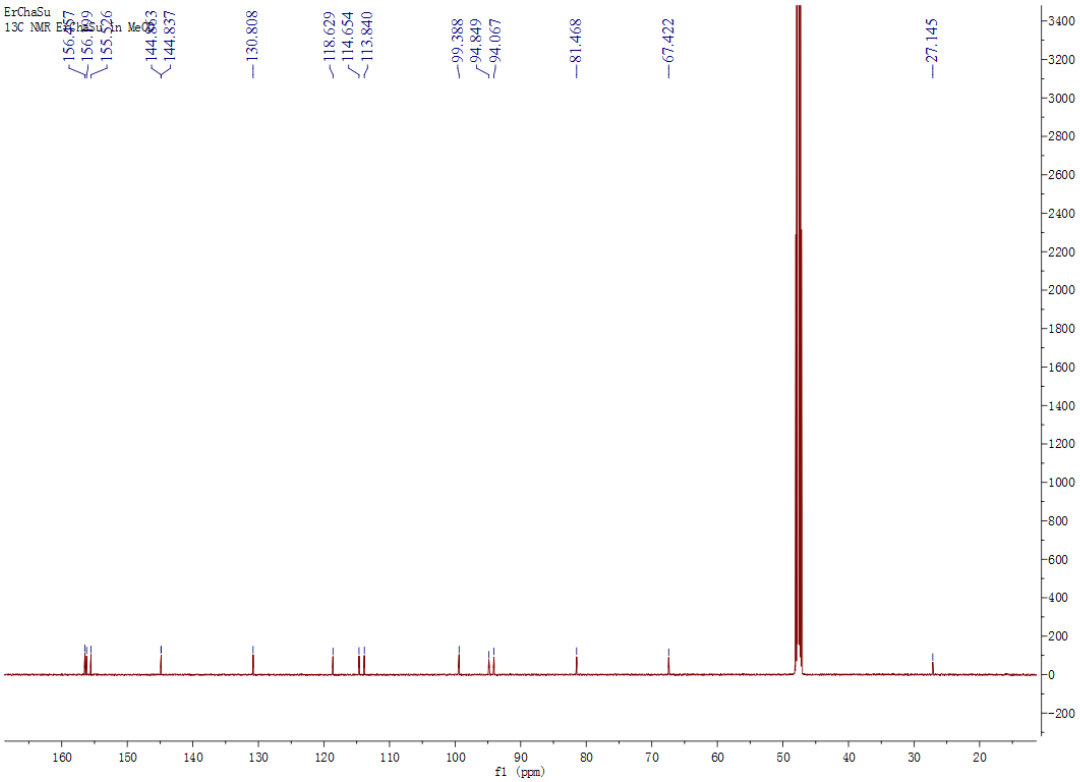

Fig. S54. ^{13}C-NMR spectrum of **CA**.

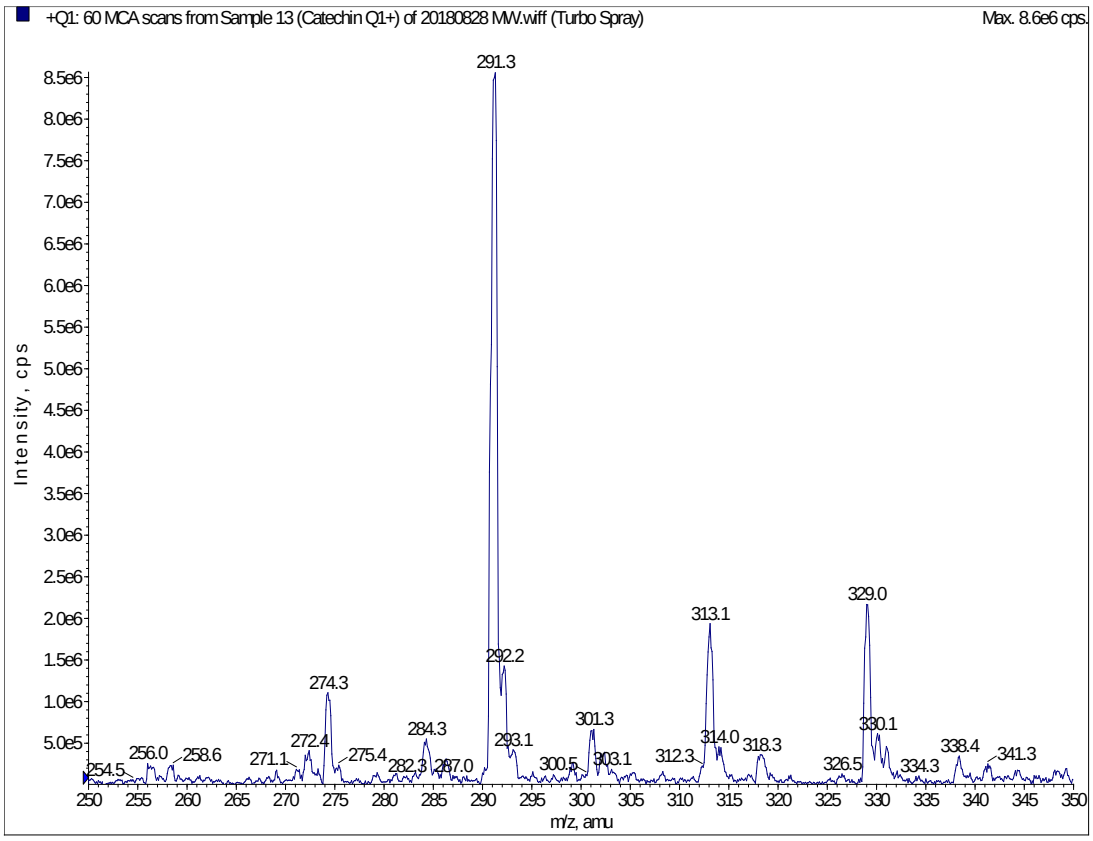

Fig. S55. (+)-ESI-MS of **CA**.

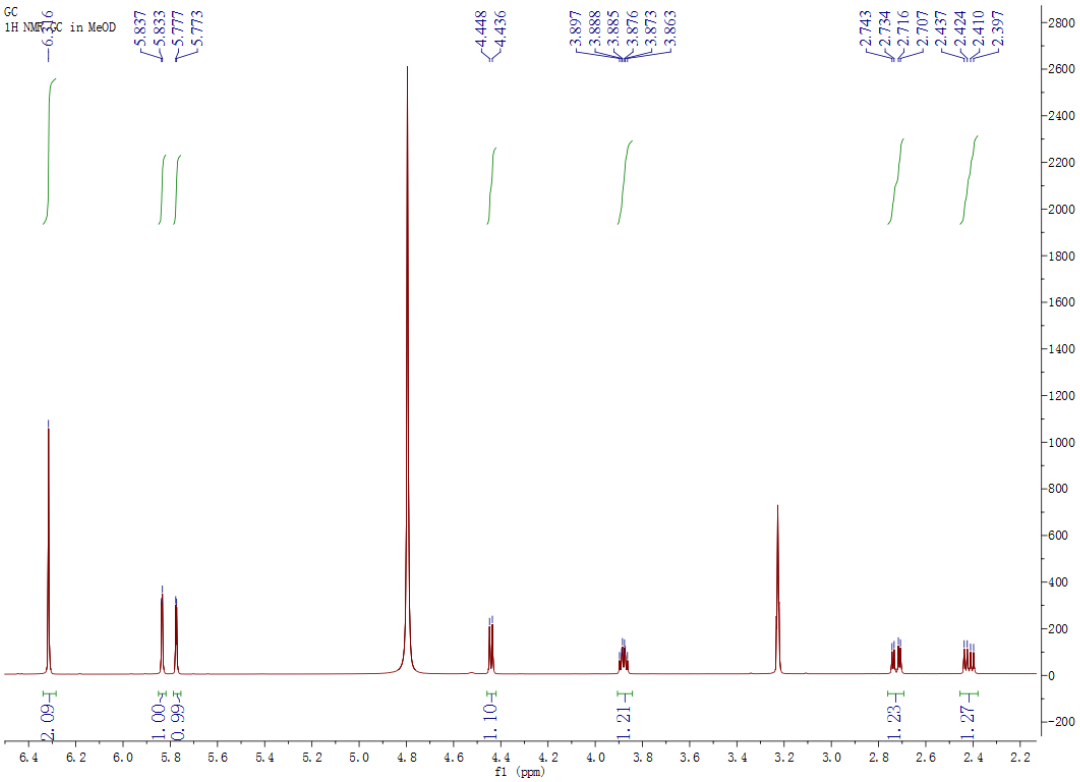

Fig. S56. ^{1}H-NMR spectrum of **GC**.

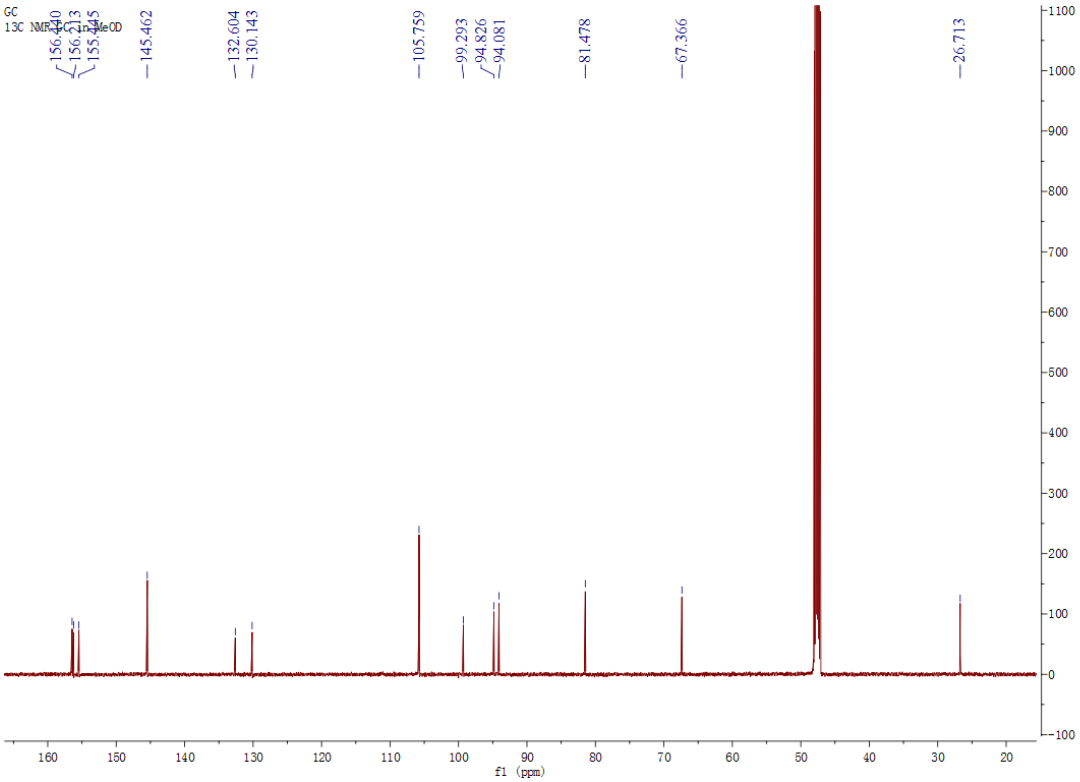

Fig. S57. ^{13}C-NMR spectrum of **GC**.

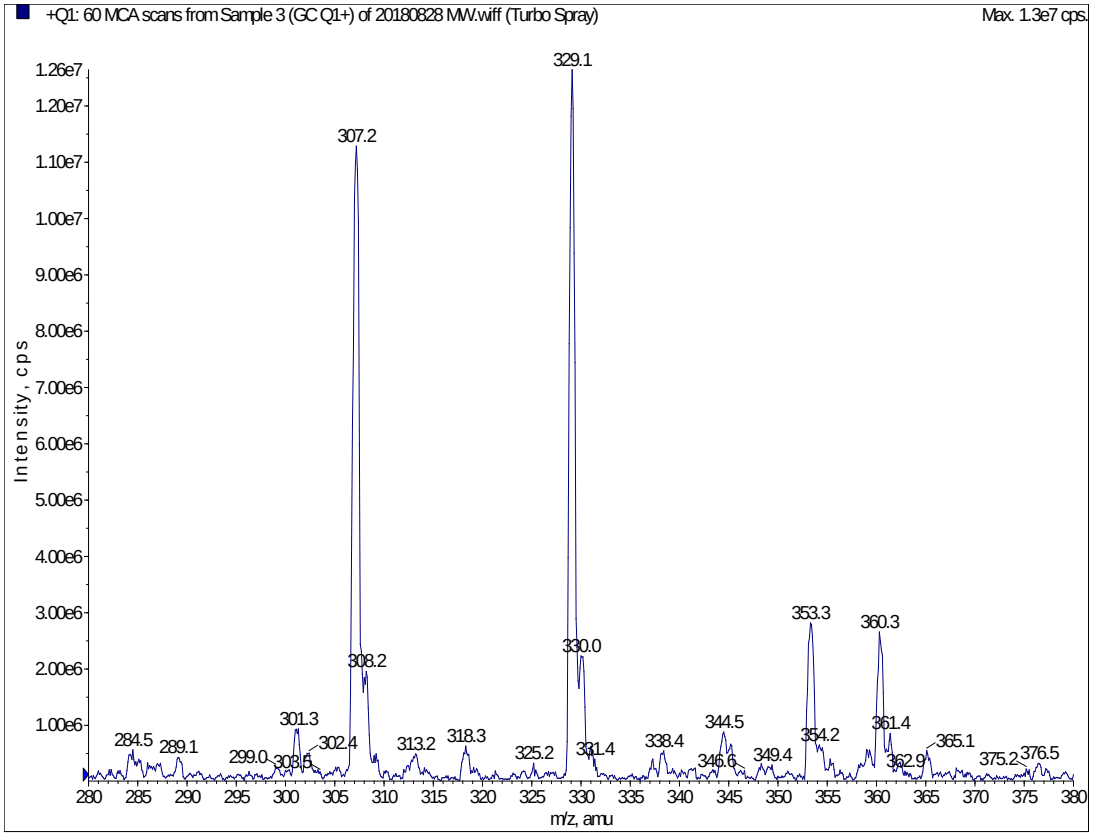

Fig. S58. (+)-ESI-MS of **GC**.

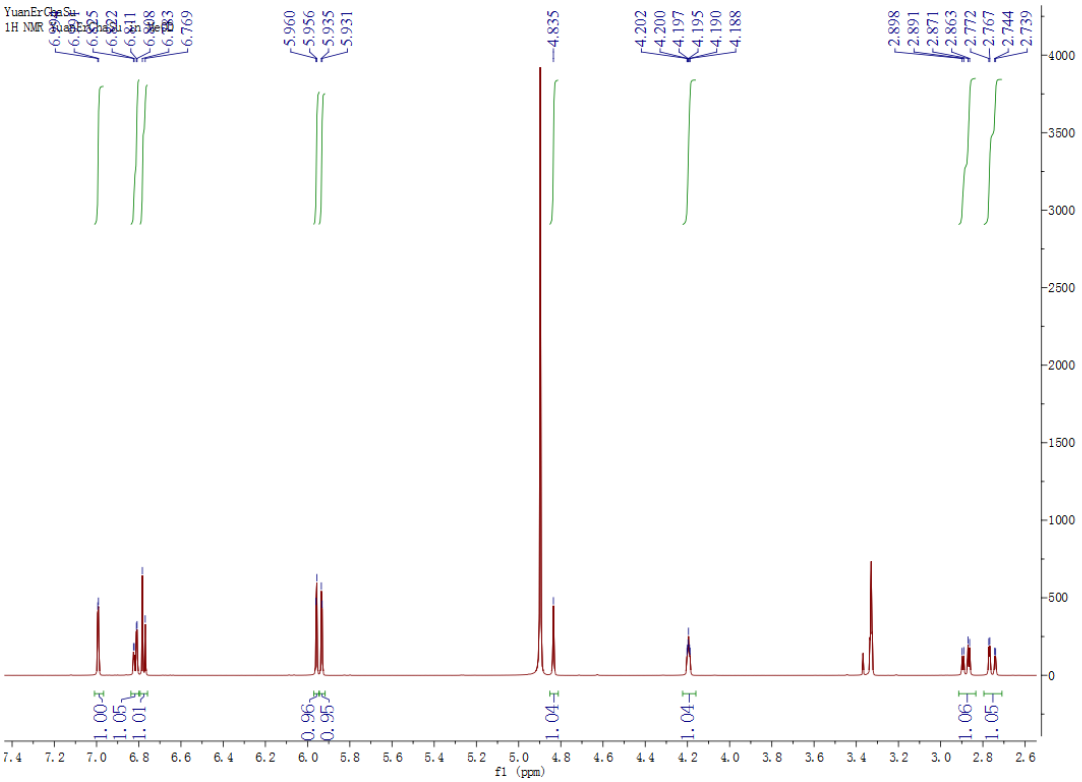

Fig. S59. ^{1}H-NMR spectrum of **ECA**.

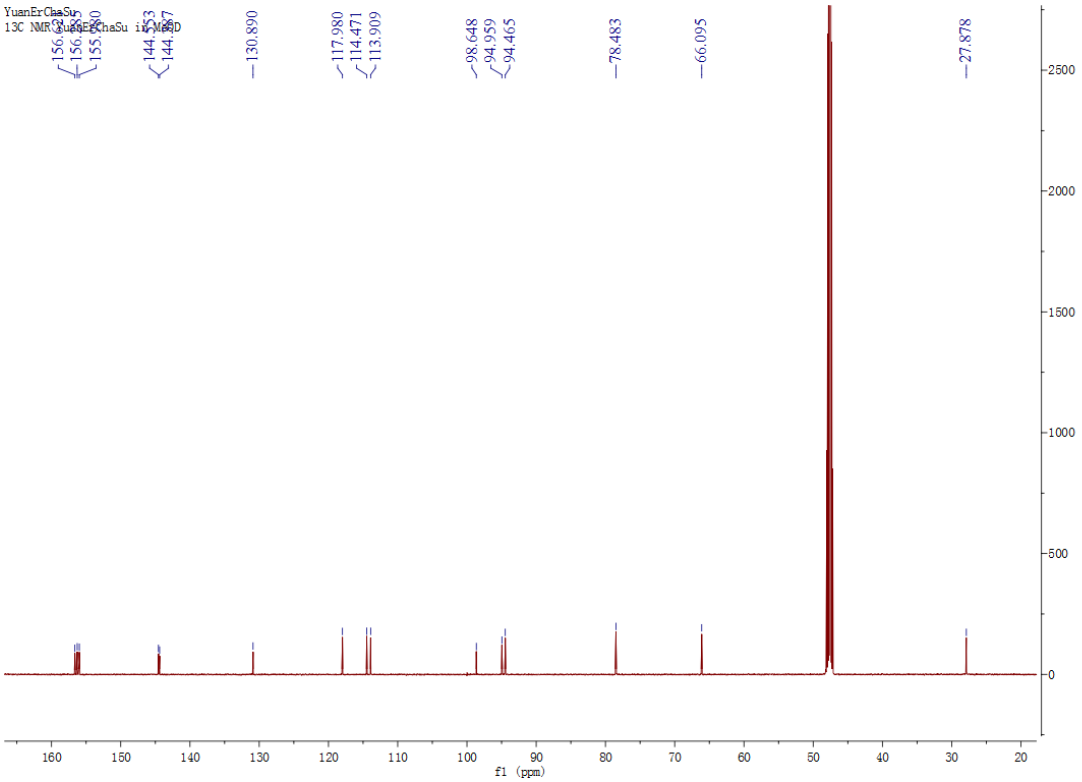

Fig. S60. ^{13}C-NMR spectrum of **ECA**.

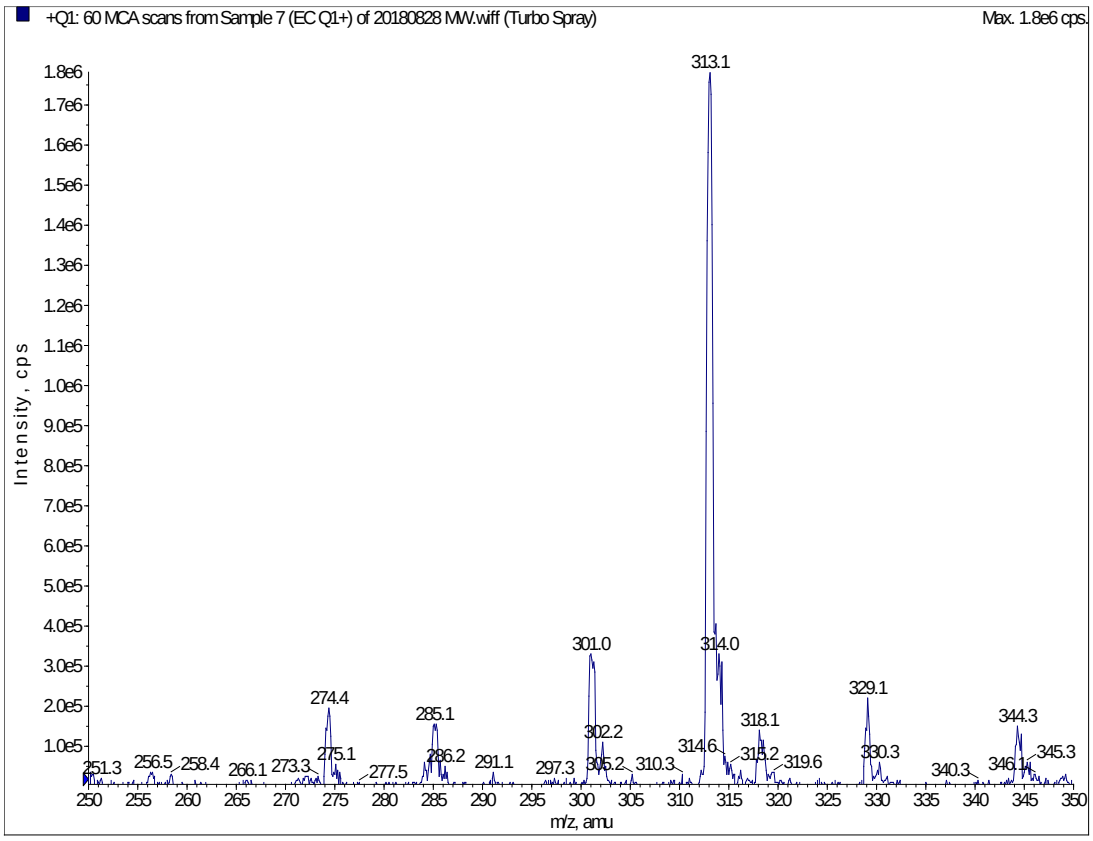

Fig. S61. (+)-ESI-MS of **ECA**.